Jennifer Christin Kahlhofer, BSc

Hepatic p53 in the Regulation of Autophagy

MASTERARBEIT

zur Erlangung des akademischen Grades

Master of Science

Masterstudium Biochemie und Molekulare Biomedizin

eingereicht an der

Technischen Universität Graz

Betreuer

Dr. Andreas Prokesch

Institut für Zellbiologie, Histologie und Embryologie

Medizinische Universität Graz

Graz, März. 2017

EIDESSTATTLICHE ERKLÄRUNG

Ich erkläre an Eides statt, dass ich die vorliegende Arbeit selbstständig verfasst, andere als die angegebenen Quellen/Hilfsmittel nicht benutzt, und die den benutzten Quellen wörtlich und inhaltlich entnommenen Stellen als solche kenntlich gemacht habe. Das in TUGRAZonline hochgeladene Textdokument ist mit der vorliegenden Masterarbeit identisch.

Datum

Unterschrift

Contents

Acknowledgments

First, I would like to gratefully and sincerely thank my supervisor Dr. Andreas Prokesch for his guidance, support, and most importantly patience during my Master studies. I have been extremely lucky to have a supervisor who always encouraged me in my ideas and slowed me down when I got too excited and nerdy. His positive outlook and trust in me inspired me and gave me the confidence to pursue a science research career. Moreover, he allowed me to do research on a topic for which I am truly passionate. For everything you have done for me, I thank you.

I would like to thank Christoph, Lissi, Petra and Sabine for helping me out in every possible way. They patiently taught me all laboratory techniques and built me up when I an experiment went wrong (which was quite often). I am fortunate to gain you as friends. And a special thanks to Sarah!

I would also like to thank all members of the Institute of Cell Biology, Histology and Embryology who supported me during my Master studies, as well as the AUTOPHAGY group at the University of Helsinki. It was an honor to be part of your team.

Finally, and most importantly, I would like to thank my parents for their encouragement and patience. I am immensely grateful for your faith in me and for allowing me to be as ambitious as I wanted. I cannot thank you enough for your constant love and support.

Abbreviation

ACTB	Beta-Actin
AICAR	5-Aminoimidazole-4-carboxamide ribonucleotide
AML-12	Alpha mouse liver 12
AMP	Adenosine monophosphate
AMPK	AMP– activated protein kinase
ATG	Autophagy related genes
ATP	Adenosine triphosphate
BCA	Bicinchoninic acid assay
BSA	Bovine serum albumin
CMA	Chaperone-mediated autophagy
Ctrl	Control
DMEM	Dulbecco's Modified Eagle Medium
DMSO	Dimethylsulfoxide
DRAM	DNA damage regulated autophagy modulator
EBSS	Earle's Balanced Salt solution
ER	Endoplasmic reticulum
GA	Glutaraldehyde
GAPDH	Glyceraldehyde 3-phosphate dehydrogenase
GFP	Green fluorescence protein
HPV	Human papillomavirus
HRP	Horseradish peroxidase
HTC16	human colorectal cancer cells
IGF-1	Insulin-like growth factor 1
LC3	Microtubule-associated protein 1A/1 B-light chain 3
MDM2	mouse double minute homologue
MOMP	Mitochondrial outer membrane permeabilization
mTOR	Mammalian target of rapamycin
mTORC1	mammalian Target of Rapamycin complex 1
MVB	multivesicular bodies
P70S6K	Ribosomal protein S6 kinase
PAGE	Polyacrylamid-gel electrophoresis
PBS	Phosphate buffered saline
PE	Phophatidylethanolamine
PFA	Paraformaldehyde
PI	Phosphatidylinositol
PI3KC3	class III phosphatidylinositol 3-kinase complex
PI3P	Phosphatidylinositol 3-phosphate
PI3P	phosphatidylinositol 3-phosphate
qPCR	Quantitative polymerase chain reaction
Rcf	Relative centrifugal force
ROS	Reactive oxygen species
RT	Room temperature
SDS	Sodium dodecyl sulfate
SEM	Standard error of mean

Sirt1	Silent information regulator T1
STV	Starvation period
TBS	Tris-buffered saline
TBS-T	TBST Tween
TFG alpha	Transforming growth factor alpha
TSC2	Tuberous Sclerosis Complex 2
UPS	Ubiquitin proteasome system
WT	Wild-type
FA	Fatty acids

Abstract

The transcription factor p53, also known as „the guardian of the genome “, is one of the best characterized tumor suppressors. P53 acts as a key component in the cellular stress response machinery and can be activated by a variety cellular stress stimuli. Here, we found that starvation induced the accumulation of p53 protein in HepG2 and primary human hepatocytes. This effect was most likely due to post-transcriptional modifications, since p53 gene expression was not increased upon starvation. Multiple cellular stressors, including starvation, can also stimulate autophagy. Indeed, autophagic flux was increased after 24h starvation in HepG2 cells and the knockout of p53 caused defective autophagic flux. We further demonstrated that p53 transcriptionally down-regulates LC3 upon prolonged nutrient deprivation. Thus, these results provide evidence of the possible link between autophagy and p53 signaling.

1 Introduction

1.1 The role of p53 as a key component in the cellular stress response

The protein p53 is one of the best characterized tumor suppressors and acts as a major barrier against cancer. The importance of p53 is most evident under conditions of cancer development. More than 50% of human cancer types harbor p53 *(TP53)* mutations, whereas inheritance of one mutant *TP53* allele significantly increase cancer risk, a condition known as Li-Fraumeni syndrome [1]. p53 prevents tumor development by serving as a key component in the cellular stress response. Numerous intrinsic and extrinsic stress signals, including malignant transformations, can activate p53. Once activated, p53 mostly functions as a transcription factor and selectively stimulates the transcription of many protein-coding and non-protein-coding genes. The result of the p53-mediated response is context-specific and depends on the cell and tissue type, intensity and type of stress. Severe stress, including genotoxic damage, drives irreversible programs of apoptosis or senescence resulting in effectively elimination of irreparably damaged or malignant cells. On the other hand, mild stress, such as increased reactive oxygen levels, leads to temporary cell-cycle arrest or decrease in proliferation. This allows the cells to survive until the damage has been repaired or the stress has been removed [2].

The classical model for p53 regulation includes p53 stabilization and activation via several post-translational events, DNA binding and selective transcription of a set of target genes. Under normal conditions, when the cell is not exposed to stress, p53 protein levels are kept low by its predominant negative regulator mouse double minute homologue (Mdm2). Mdm2 is an E3 ubiquitin ligase and prevents p53 function through the ubiquitin-proteasome pathway. Stress-induced initial stabilization of p53 occurs through post-translational modifications which seems to interfere with the Mdm2-p53 interaction. Disruption of the Mdm2-p53 interaction leads to activation and accumulation of p53 in cells [3]. Then, activated p53 can transfer into the nucleus, where it works as transcription factor and selectively induces the expression of target genes. However, p53 can also regulate different pathways via direct protein-protein interactions. For instance, it has been shown that p53 interferes with the Bcl-2 family at the mitochondria membrane to induce apoptosis [4]. However, it has also been suggested that both, nuclear and cytoplasmic p53, regulates apoptosis [5]. Furthermore, it has been proposed that p53 also functions in homologous recombination and microRNA processing. [6, 7]. Because these various responses of p53 are essential to maintain genomic integrity and preventing cancer development, p53 is also known as “guardian of the genome” [8].

1.2 p53 and its impact on metabolism

Alterations in the metabolism have been regarded as hallmark for tumor progression and contributes to cancer development. Because of its crucial role in tumor suppression, it is not surprising that p53 also regulates cancer cell metabolism. It has been shown that p53 coordinates various metabolic changes in cancer cells, including the regulation of glycolysis [9], mitochondrial oxidative phosphorylation [10], pentose phosphate pathway [11], and lipid metabolism [12].

To meet energetic demands of rapid growing and dividing cells, cancer metabolism shifts to aerobic glycolysis, known as Warburg effect. Aerobic glycolysis provides energy at a fast rate and intermediates from glycolysis can serve as precursors for macromolecule biosynthesis [13]. True to its role as tumor suppressor, it has been described that p53 counteracts the Warburg effect by restricting glycolysis and enhancing oxidative phosphorylation [9].

In addition, p53 signaling also regulates lipid metabolism in cancer cells [14]. Lipids are important for biosynthesis of membranes, are used as second messengers for signal transduction, and serves as source of energy during nutrient deprivation [12, 13]. Thus, reprogramming of lipid metabolism ensures cancer cell survival. p53 has been demonstrated to negatively regulate lipid synthesis by inhibiting fatty acid synthesis and inducing fatty acid oxidation [2]. Furthermore, enhanced fatty acid oxidation can inhibit glycolysis [14]. Hence, regulation of metabolic pathways may serve as another mechanism by which p53 prevents cancer development [15].

1.2.1 p53 is activated by metabolic stress

Beyond its tumor suppressor properties, it has been shown that p53 is also activated by metabolic stress in non-transformed cells. It is now appreciated that p53 has a more complex role as cellular stress sensor and is also involved in metabolic diseases [14]. For instance, it has been previously reported that p53 was induced in mice models of fatty liver disease, indicating the involvement of p53 in the mechanism of hepatocellular injury [16]. Further studies also revealed a link between p53 and atherosclerosis. They showed that the absence of p53 led to larger atherosclerotic plaques in mice, mostly due to increased cell proliferation in atherosclerotic lesions [17]. However, a key problem with much of the literature on p53 signaling in cell metabolism is, that most of these metabolic studies were done in germline or early embryonic p53 loss-of functions models that are prone to cancer development. Schupp et al. recently showed that p53 signaling was associated with metabolic changes upon nutrient deprivation in adipose tissue, liver, and skeletal muscle of wildtype mice, suggesting a role of p53 in response to starvation [18].

1.3 Autophagy in response to nutrient starvation

Macroautophagy (hereafter autophagy) is an important and evolutionary conserved lysosomal pathway responsible for the bulk-degradation of cytoplasmic material such as cytosol, protein aggregates and organelles. It regulates adaptive responses to starvation and various other extrinsic and intrinsic stresses in order maintain intracellular homeostasis [19].

1.3.1 Autophagy initiation is under the control of multiple signaling events

Autophagy initiation is driven by the concerted action of autophagy-related proteins (ATG) **(Fig 1).** Once induced, the autophagic machinery starts to form an isolation membrane in a *de novo* manner, also known as phagophore. The recruitment of ATG proteins and lipids expands the membrane to form a double-membrane vesicle, called autophagosome [20]. Different ATG-proteins are known to be involved in autophagosome formation. However, the origin of the lipids that contribute to autophagosome membrane are still a topic of debate. It has been shown that the endoplasmic reticulum-mitochondrial contact site has an important role in starvation-induced autophagy [23], while also lipids from the Golgi and plasma membranes seems to be involved [21, 22].

One of the first detectable events in autophagy initiation is the formation of the ULK1/2 kinase complex. ULK1/2 activity is controlled by mammalian target of Rapamycin complex 1 (mTORC1), which is a central inhibitor of autophagy. Under normal conditions, mTORC1 inactivates ULK1/2 by phosphorylation and therefore prevents autophagy induction. The class III phosphatidylinositol 3-kinase (PI3KC3) complex is important for the nucleation and assembly of the initial phagophore membrane. Activation of this complex leads to the localized phosphorylation of phosphatidylinositol (PI) to generate phosphatidylinositol 3-phosphate (PI3P) in the membranes of elongating phagophores [24], which seems to stabilize ULK1 and recruit further factors [25].

After nucleation, the phagophore recruits ATG12, which is covalently bound to ATG 5, and ATG16L1 [26]. This conjugation system forms large oligomers and is essential for the elongation of the phagophore membrane [27]. Upon elongation of the phagophore, the microtubule associated protein 1 light chain 3 (LC3) undergoes post-translational modification, including the cleavage of the carboxyl terminal region of proLC3 to form the cytoplasmic form, LC3-I. The ATG12-ATG5 conjugations system then promotes the transfer of LC3-I to the head group of the membrane lipid phosphatidylethanolamine (PE) to create LC3-II. Upon closure of the phagophore, the ATG12-ATG5/ATG16L1 complex dissociates from the membrane while part of the lipidated LC3-II is bound to the inner limiting membrane of autophagosome. Thus, LC3-II is a prominent marker of autophagosome formation [28, 27].

1.3.2 Mature autophagosomes fuse with lysosomes

The step-wise progression of autophagosome formation leads to the sequestration of cytoplasmic components and organelles. Finally, autophagosomes fuse with lysosomes to form autolysosomes [20]. Alternatively, it has been shown that autophagosomes first fuse with multivesicular bodies (MVB) to form amphisomes, prior to fusion with lysosomes [29]. Thus, maturation of autophagosomes in mammalian cells is thought to be a multi-step process including several fusion events with early and late endosomes as well as lysosomes. During maturation, the autophagosomes become acidic. It is thought that this acidification is due to fusion with endosomes or other autophagic vacuoles. Direct fusion of autophagosomes with lysosomes then delivers the sequestered cargo, still enwrapped by the inner limiting membrane, into the lysosomal lumen. Both, the autophagic cargo and the membrane around it, are then degraded inside lysosomes by lysosomal hydrolases. Subsequently, the degraded products are transported back to the cytoplasm to provide nutrients for biosynthesis and to support cellular metabolism [30]. As mentioned in the previous paragraph, lipidated LC3-II is bound to autophagosomal membranes and is also degraded by lysosomal proteases. Thus, the turnover of LC3-II proteins reflects autophagic activity and is used to monitor autophagy [31].

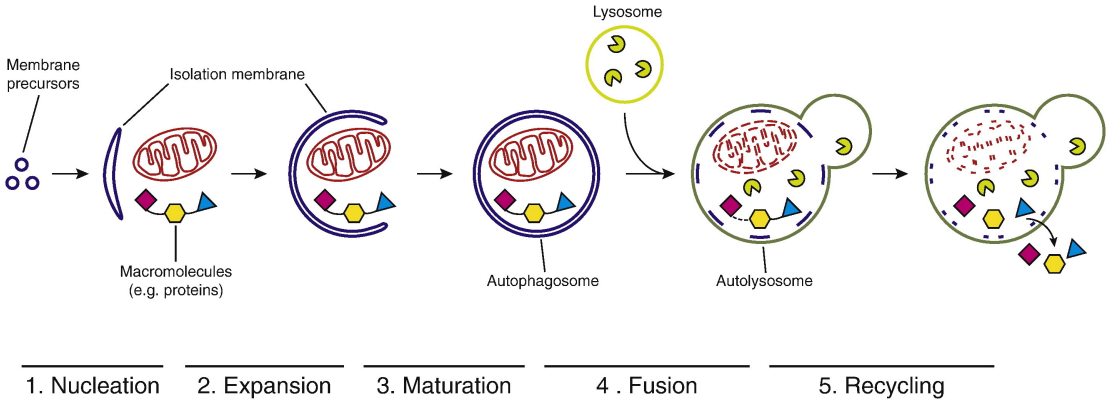

Figure 1: Schematic presentation of autophagy initiation. **(1)** Membrane precursors begin to form an isolation membrane in a *de novo* manner **(2)** The isolation membrane expands and enwraps cytoplasmic cargo **(3)** Isolation membrane close to give rise to a mature double-membrane autophagosome **(4)** The outer autophagosomal membrane fuses with vesicles from the endosomal/lysosomal compartments, leading to the degradation of the inner membrane and the cargo **(5)** Degradation products are recycled back into the cytoplasm. Adopted from *Zaffagnini et al* [19]

1.3.3 Autophagy in the liver

Autophagy is an important degradation process that ensures optimal functioning of eukaryotic cells [32]. It regulates the digestion and recycling of long-lived proteins, large macromolecules and organelles that have become damaged or aged. One important role of autophagy is to recycle non-essential parts of the cell during starvation [33]. In animals, it has been shown that starvation induces the largest protein degradation in the liver as compared to other organs [34].

In addition, basal level of autophagy is important for cellular homeostasis by preventing the accumulation of dysfunctional organelles and proteins. The rapid induction of autophagy to cellular stress further emphasize its cytoprotective function. The autophagic flux contribute to adaption and survival of the cells in response to cellular stress. Moreover, the degradation pathway is involved in the clearance of invading microorganisms and toxic protein aggregates and therefore plays an important role during infection and in aging. [35].

The relevance of functional hepatic autophagy is most evident in metabolic disorders which lead to altered autophagy. It has shown that blockage of basal autophagy is associated with hepatomegaly, which is followed by inflammation, hepatitis and tumorigenesis [36] During periods of fasting, autophagy maintains liver homeostasis through recycling of amino acids, which are then used for gluconeogenesis and ketone body formation. Liver autophagy is also important for the regulation of plasma glucose concentrations in neonates during fasting [37]. In addition, lipids stored in lipid droplets are degraded by selective autophagy (lipophagy) to release fatty acids. Those can be oxidized in mitochondria to supply the cell with ATP [38].

1.4 The dual role of p53 in the regulation of autophagy

Autophagy is essential for the long-term survival of cells and induced by various stress stimuli including DNA damage. It has been shown that multiple oncogenes associates with autophagy induction, suggesting a link between autophagy and cancer development. These findings indicate that basal autophagy may harbor tumor suppressor features. Conversely, enhanced autophagy may contribute to tumor cell survival during tumor progression [39].

Since p53 is one of the most prominent tumor suppressors and key component of the cellular stress response, it is not surprising, that p53 signaling is also involved in the regulation of autophagy. P53 activation can be induced by a variety of stimuli, including genotoxic and oncogenic stress, inducing p53-dependent transcription of pro-autophagy target genes. Accumulating evidence indicates that p53 stimulates autophagy by the inhibition of its negative regulator, the mTORC1 complex. For instance, p53 transactivates components of the AMP-activated protein kinase (AMPK) complex, a conserved cellular sensor for energy levels, which in turn downregulates mTORC1 activity. In addition, AMPK also phosphorylates p53 and hence induces cell cycle arrest under metabolic stress conditions [40]. In contrast, cytoplasmic p53 seems to suppress autophagy, although the exact mechanism is still unknown [2].

Hence, the relationship between p53 and autophagy is content-specific and differ among different cell types. Inducing autophagy under mild stress condition is essential to maintain intracellular metabolic homeostasis. Therefore, this may reduce the accumulation of cancer-promoting derangements in normal cells. In contrast, it has been shown that endogenous wildtype p53 inhibits autophagy in human colorectal cancer (HCT116) cells through the posttranscriptional downregulation of LC3. In HCT116 cells, the basal autophagic flux is high and it is assumed that the inhibition of autophagy upon starvation promote limited but sustainable levels of autophagy over time. Hence, the ability to either promote or suppress autophagy may allow p53 to maintain autophagic homeostasis by adjusting the rate of autophagy to changing circumstances [41]

1.5 Previous data: the p53 pathway is activated by fasting in liver of healthy mice

Previous research has demonstrated that p53 serves as a central regulator of fasting in mice [18]. Based on these findings, Prokesch et al. further confirmed the role of the tumor suppressor in the physiologic adaption to nutrient deprivation. The study revealed a robust increase in liver p53 protein in mice, which were fasted for 24 h, in comparison to mice which were fed *ad libitum*. Moreover, p53 protein levels decreased again in mice which were fasted for 24h and

refed for 2 h **(Fig. 2 A)**. However, this p53 accumulation was not due to up-regulation of p53 gene expression or down-regulation of the mRNA of its negative regulator Mdm2, which mediates p53 degradation **(Fig. 2 B).** These data demonstrated that the accumulation of hepatic p53 in mice was most likely due to posttranscriptional modifications. In addition, it was shown that p53 stabilization was mediated by an AMPK-dependent mechanism.

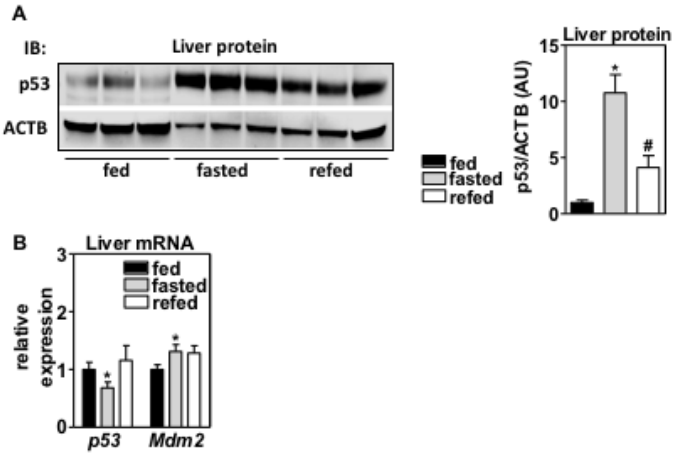

Figure 2: p53 protein is stabilized in liver in fasted mice. Four-month-old C57BL/6N mice were either fed ad libitum, starved for 24h, or fasted and subsequent refed for 2h. **(A)** Western Blot analysis were performed to detect p53 protein in fed, starved and refed mice. Expression of ß-actin (ACTB) was used as loading control. **(B)** qPCR of RNA extracted from shock-frozen mice liver samples were used to determine p53 and MDM2 mRNA levels.

Taken together, these findings indicate a novel function of p53 activity in the physiological adaption to starvation in liver [42]. It was therefore of interest to investigate whether starvation also increases p53 protein levels *in vitro*. Further, this experiment raised many questions about the consequences of p53 accumulation upon starvation. A review of Kroemer et al in 2010 proposed a dual role of p53 in the control of autophagy [40]. However, the role of starvation-induced autophagy in hepatocytes is barely investigated.

1.6 Aim of the study and project design

This master thesis is based on recently published studies of Prokesch et al., in which mouse studies revealed a novel role of the tumor suppressor p53 as a central regulator of liver metabolism during feeding-fasting transitions [42]. The aim of this thesis was to confirm the observed findings *in vitro*. Therefore, different hepatocyte model systems were used to test the impact of nutrient deprivation on p53 expression. The outcome was investigated by quantitative gene expression analysis and biochemical assays. In addition, it was questioned whether p53 stabilization interplay with fasting-induced autophagy in hepatocytes. Thus, p53-expressing and p53-deficient HepG2 cells were used to investigate the role of p53 on autophagy regulation upon nutrient deprivation.

A second approach focused on the analysis of autophagy *in vivo.* Traditional ultrastructural analysis using electron microscopy was used to analyze autophagic vesicles in liver sections of wild-type and p53-deficent mice with and without starvation. This part of this master thesis was done during an internship in the Autophagy group at the Department of Biosciences under the supervision of Eeva-Liisa Eskelinen at the University of Helsinki.

2 Materials

1) Biological material

Used cell lines are listed in table 1.

Table 1. cell line models

Alpha mouse liver 12 (AML-12)	**ATCC**
Mus musculus, source: liver of CD1 strain, line MT42)	
Primary human hepatocytes	**QPS Hepatic Biosciences, USA**
Homo sapiens, source: liver of nondiseased male	
HepaRG	**Invitrogen**
Homo sapiens, source: hepatic progenitor cell line derived from female donor	
HepG2	**ATCC**
Homo sapiens, source: liver hepatocellular carcinoma cells of 15 years old male	
Upcyte Hepatocytes	**Upcyte Technologies GmbH**
Homo sapiens, source: liver of nondiseased female, 9 years old	

2) Growth medium for cell culture

All cell culture reagents were purchased from Invitrogen and listed in table 2.

Table 2. growth medium for mammalian cell lines

AML-12	DMEM/F + 1x L-Glutamin + 1% Penicillin/Streptomycin (PS) + 10% Fetal Bovine Serum (FBS) + 10 nM HEPES
AML-12: working solution (40 ml)	Stock solution + 1 mM dexamethasone + ITS (insulin, transferrin, selenium, 100x)
HepG2 high glucose	DMEM: 4,5 g/L L-glucose + 10% FBS + 1% PS
HepG2 low glucose	DMEM: 1,0 g/L L-glucose + 10% FBS + 1% PS
Starvation medium	HBSS + 1 M HEPES

3) General buffers

General buffers used in the various methods are listed in table 3.

Table 3: general buffers

Lysis buffer (RIPA): Stock solution	150 mM NaCl 2 mM EDTA 50 mM NaF 0,1% SDS 0,5% Na-deoxycholate 1% NP-40 50 mM Tris-HCl, pH 7,2
RIPA buffer: working solution	RIPA buffer + 1x protease inhibitor + 1x phosphatase inhibitor
10x TBS-Buffer, pH 7,4	121,1 g Tris 175,32 g NaCl + 2000 ml dH2O
1x TBS-T buffer	10 ml 10x TBS + 500 µl Tween20 + 990 ml dH2O
1x TBS-buffer	10 ml 10x TBS + 990 ml dH2O
Blocking buffer (Western Blot) and dilution for antibodies	1,5 g skimmed milk powder + 30 ml TBS-T

4) Reagents

Concentrations of different reagents are listed in table 4.

Table 4: concentrations and dilutions of used reagents

AICAR dissolved in dH2O	Stock solution: 1mM Working solution: 250 nM
Nutlin-3a dissolved in DMSO	Stock solution: 10 mM working solution: 10 µM
Bafilomycin A1 dissolved in DMSO	Stock solution: 10 µM working solution: 10 nM
Rapamycin dissolved in DMSO	Stock solution: 100 µM working solution: 100 nM

5) Kits

Used kits are listed in table 5.

Table 5: commercial kits

Pierce ™ BCA Protein Assay Kit	Thermo Fisher Scientific
SYBR® Green Master Mix	BioRad
PeqGOLD cDNA Synthesis Kit H Plus	Peqlab
PeqGOLD total RNA kit	Peqlab

6) Primers

All primers used in this thesis are listed in table 6.

Table 6: Sequences of specific primer pairs

Target Gene	Primer	Sequence (5'-3')
GAPDH	forward reverse	ACCCACTCCTCCACCTTTGA CTGTTGCTGTAGCCAAATTCGT
TP53	Forward Reverse	CAGCACATGACGGAGGTTGT TCATCCAAATACTCCACACGC
CDKN14 (p21)	Forward Reverse	GGCAGACCAGCATGACAGATT GCGGATTAGGGCTAACACTTTGT
DRAM-1	Forward Reverse	TCAAATATCACCATTGATTTCTGT GCCACATACGGATGGTCATCTCTG
TSC2	Forward Reverse	CCAAACCAACAAGCAAAGATTCA CACATTCCATGCTCAGTTCTCT

7) Antibodies

All antibodies used in this study are listed in table 7.

Table 7: Antibodies used for Western Blotting

Antigen (specification)	Host	Dilution 1st antibody	Company and Cataloge Nr
ß-Actin (AC-15)	Mouse	1:250000	Abcam #ab6276
P53-DO1	Mouse	1:2000	Cell Signaling #sc-126
LC3B/MAP1	Rabbit	1:1000	NOVUS #NB100-2220
P62 (SQSTM1)	Rabbit	1:1000	Sigma-Aldrich #P0067
p-P70-S6K1 (Thr398)	Rabbit	1:500	Cell Signaling #9234

3 Methods

3.1 Cell Culture and Treatments

All cell culture techniques were performed under sterile conditions at any time.

3.1.1 Cell culture of AML-12 cells

Alpha mouse liver 12 (AML-12) hepatocytes were cultured in DMEM/F (Gibco) containing 0,005 mg/ml insulin, 0,005mg/ml transferrin, 5 ng/ml selenium, and 40 ng/ml dexamethasone with 10% fetal bovine serum and 1% penicillin/streptomycin (all Thermo Fisher Scientific) in a humidified atmosphere containing 5% CO_2 at 37°C. The cells were cultured in 75 cm^2 cell culture flasks (Sarstedt) until they reached 70-80% optical confluence. For passaging, the medium was removed and the cells were washed with 5 ml 1x PBS. 2ml of Accutase (BioWest) was then added and incubated at 37°C, allowing the cells to detach for 5 min. 2ml culture medium was added and the cell suspension was centrifuged at 1200 xg for 5 min. Cells were counted and seeded in 12-well plates (1.0 x 10^6 cells/ml and 1.0 x 10^5 cells/ml) for starvation experiments.

3.1.2 Cell culture of primary human hepatocytes

Primary human hepatocytes from two male nondiseased donors were thawed and seeded according to the manufacturer's instructions (QPS Hepatic Bioscience). Briefly, cells were thawed in 50 ml Cryopreserved Hepatocyte Recovery Medium, centrifuged at 100xg for 8 min and resuspended in Cryopreserved Hepatocyte Plating Medium. 0,8 x 10^6 cells/ml were plated in collagen I-coated 24-well plates (BD biocoat). 24 hours after plating, the medium was changed to Cryopreserved Hepatocyte Maintenance Medium (all QPS Hepatic Bioscience). Three days after plating, cells were washed with PBS and incubated with starvation medium starting the experiment.

3.1.3 Cell culture of HepaRG

Cryopreserved differentiated HepaRG cells were thawed and seeded according to the manufacturer's instructions (Invitrogen, Thermo Fisher Scientific). Briefly, cells were thawed in HepaRG Thaw, Plate & General Purpose Working Medium resulting in a 1:10 ratio of cell suspension to total volume. Cell suspension were centrifuged at 400xg for 2 min. 0,6x10^6 viable cells/well were plated in collagen I-coated 24-well plates (BD biocoat). 24 hours after plating, the medium was changed to HepaRG Maintenance/Metabolism Working Medium and cultured at 37°C with 5% CO_2 atmosphere for 7 days. HepaRG Maintenance/Metabolism Working Medium (all Thermo Fisher Scientific) was renewed at day 5 and day 7 after thawing. On day 8, medium was removed and changed to starvation medium, starting the experiment. HepaRG working medium were prepared by adding the HepaRG Supplement (Thawing, Plating & General Purpose Working Medium; Maintenance/Metabolism Working Medium) with William's Medium E and GlutaMAX (Invitrogen, 1:100 dilution).

3.1.4 Cell culture and treatment of Upcyte Hepatocytes (upregulated hepatocytes)

Cryopreserved Upycte Hepatocytes cells were thawed and seeded according to manufacturer's instructions (Upcyte technologies) with slight deviations to our settings. Briefly, cells were thawed in 50 mL Hepatocyte Thawing Medium and centrifuged at 100xg for 5 min. Cells were re-suspended in 5ml High Performance Medium (all Upcyte Technologies). For sub-culture, the cells were seeded at 10.000 cells/ cm^3 in a collagen coated T75-flask until they reached 70-80% confluence. Medium was renewed every third day. 8 days after seeding, cells were

passaged by using 1x Trypsin (0,05%/0,02% EDTA). To stop the Tryspin activity, High Performance Medium containing 10% fetal bovine serum was added. Cells were centrifuged at 100xg for 5 min and seeded at 80.000 cells/cm^2 in High Performance Medium in a collagen type I coated 12-well plate. The cells were then cultured for three days following starvation experiments on day 15.

3.1.5 Cell culture of HepG2 cells

The human hepatocellular carcinoma cells were cultured either in DMEM (Gibco) containing 1 g/L L-glucose (low glucose medium) or DMEM containing 4,5 g/L L-glucose (high glucose medium) with 10% fetal bovine serum and 1% penicillin/streptomycin in a humidified atmosphere containing 5% CO_2 at 37°C. (all purchased form Thermo Fischer Scientific). The cells were cultured in 75 cm^2 cell culture flasks until they reached 70-80% optical confluence. Subsequently, the medium was removed and the cells were washed with 5 ml 1x PBS. 2ml of Accutase was then added, following incubation at 37°C for 5 min, allowing the cells to detach. Then, 2ml culture medium was added and the cell suspension was centrifuged at 1200 x g for 5 min. For passaging, the appropriate amount of cell suspension was added to a new flask (75 cm^2). HepG2 cells were passaged every 3-4 days. For starvation experiments, 1.0 x 10^6 cells/ml were seeded into a 12-well culture plate.

3.1.6 Cell culture and treatment of HepG2 Clone 7 cells

The stable p53 knockout (KO) HepG2 cells were a generous gift of Christoph Nössing, Institute of Cell Biology, Histology and Embryology, Medical University Graz. Cells were cultured and maintained in DMEM containing 4,5 g/L L-glucose (high glucose medium) with 10% fetal bovine serum and 1% penicillin/streptomycin in a humidified atmosphere containing 5% CO_2 at 37°C. All cell culture procedures were done following the instructions for HepG2 cells.

3.2 Protocol for starvation-mediated p53 stabilization in vitro

For starvation experiments, cells were seeded in 12-well plates according to their recommended seeding density. The cell number was determined by CASY cell counting technology and by Trypan blue exclusion. Growth medium was changed daily until the cells reached 100% optical confluence to avoid cell cycle effects. Subsequently, maintenance medium was removed and the cells were carefully washed with 500µl 1x PBS. Then, cells were cultured in either starvation medium consisted of 1x HBSS and 10mM HEPES (Gibco/Invitrogen) or maintenance medium for indicated time. Autophagy inhibitor Bafilomycin A1 (Cayman Chemical dissolved in DMSO, used at 10nM), was added 2 hours prior harvest. DMSO was used as vehicle control. Cells were starved for desired time point as described. Protein and RNA were collected for further analysis.

3.3 mRNA Analysis using Real-Time PCR

3.3.1 RNA Isolation

Cells were cultured in 12 or 24-well culture plates and were collected for RNA analysis at indicated time points. The medium was aspirate and 400 µl RNA Lyisis Buffer T (PeqGOLD total RNA Kit) was added directly to the cells. The lysate was transferred into a reaction tube and vortexed for 10 sec. Total RNA was isolated by using PeqGOLD total RNA Kit (Peqlab) following manufacturer's instructions. RNA concentration was quantified spectrophotometrically with NanoDrop (Peqlab). The RNA samples were stored at -20°C until further use.

3.3.2 cDNA Synthesis

cDNA was synthetized from total RNA using cDNA-Synthese Kit H Plus (Peqlab). 1 µg of isolated RNA was used to generate first strand cDNA in a two-step RT-PCR protocol. For the first strand cDNA synthesis, following reagents were added into a sterile, nuclease-free tube on ice:

RNA	1 µg
Oligo $(dT)_{18}$ primer	1 µl
Random hexamere primer	1 µl
Water, nuclease free	To 12 µl
Total volume	12 µl

The reaction samples were heated up for 5 minutes at 65°C and placed back on ice.
Then, the following components were added to complete cDNA synthesis:

5x Reaction Buffer	4 µl
peqGOLD RNase Inhibitor (20 u/µl)	1 µl
10 mM dNTP Mix	2 µl
peqGOLD M-MuLV H Plus Reverse Transcriptase (200 u/µl)	1 µl
Total volume	20 µl

Reaction samples were incubated for 5 min at 25°C followed by 60 min at 42°C. The reaction was terminated by heating at 70°C for 5 min. PCR reactions were performed using BioRad C1000 Thermal Cycler with dual 48/48 fast reaction module. The cDNA was diluted in nuclease free water (Sigma-Aldrich) to get a concentration of 1 µg/ml and stored at -20°C.

3.3.3 Primer design and preparation of primer stock solution

Primer sequences were either adapted from literature or from the online database "PrimerBank" (Harvard Medical School, the Massachusetts General Hospital). The online tool "NCBI Primer-BLAST" was used to design primers for qPCR reactions. For efficient amplification, primers were designed to amplify a region of 100 – 200 bp. The melting temperature was kept below 65°C. To guarantee amplification of mRNA, primers were designed to span an exon-exon junction. Every primer was tested using the online tool "In-Silico PCR" (University of California, Santa Cruz) and "the mFold Web server" (The RNA Institute, College of Arts and Science, University at Albany). Primers were purchased from Microsynth and diluted according to manufacturer's instructions to a final concentration of 100 µM. For application to real-time PCR analysis, stock solutions of forward and reverse primers were mixed to achieve a final concentration of 800 nM.

Forward Primer (100 µM)	8 µl
Reverse Primer (100 µM)	8 µl
ddH_2O	984 µl
Total volume	1 ml (800 nM)

3.3.4 Quantitative Real-Time PCR

Quantitative Real-Time PCR (qPCR) was performed using the SYBR® Green Master Mix (BioRad, Hercules, CA, USA). 2,5 µl of the Primer Mix (800 nM) was added into a Mutiplate 96-well PCR plate (BioRad). Then, 2,5 µl of cDNA (1 µg/ml) was mixed with 5 µl SYBR Green Master Mix (Biorad) to complete the reaction mix. Each reaction mix consisted of:

cDNA template	2,5 µl
SYBR Green Master Mix (Biorad)	5 µl
Primer Mix (800 nM)	2,5
Total volume	10 µl

Samples were measured in duplicates. *Gapdh* was used as reference gene. The Multiplate 96-well PCR plate was sealed and centrifuged at 300xg for 1 min. The qPCR reaction was performed using a BioRad CFX cycler. Primer sequences are listed in Materials Table 6.

Cyclin protocol of qPCR:

Phase 1 -1 cycle	10 min, 95°C
Phase 2 – 40 cycles	15 sec, 95°C 1min, 60 °C 1 min, 72°C
Phase 3- 1 cycle	30 sec, 95 °C 30 sec, 60 °C 30 sec, 95°C

3.3.5 Data Analysis

qPCR data were analyzed by relative quantification using CFX Manager ™ software (BioRad). Primer specificity was checked by melt-curve analysis. Nonspecific products such as primer dimers could be detected as an additional peak in the melt-curve analysis. The data were normalized to GAPDH as internal housekeeping gene.

3.4 Immunoblotting

3.4.1 Protein Isolation

Cultured cells were washed with 1x PBS and harvested in 100 µl RIPA buffer including PIC and PhosStop (Roche) using a cell scraper. Samples were vortexed and frozen at -20°C until further processed. Cells were lysed by sonication. Cell breakdown was performed in short pulses (10 sec) at lowest intensity (1). Thereafter, samples were centrifuged at 13000 rcf at 4°C for 15 min. Supernatant was transferred into cooled reaction tubes and immediately placed on ice.

3.4.2 Determination of protein concentration

Protein concentration was determined by using the Pierce ™ BCA Protein Assay Kit (Thermo Fisher Scientific) according to manufacturer's recommendations. Protein concentrations were determined with reference to bovine serum albumin (BSA) as standard. A standard curve was generated using serial dilution of BSA (stock 2 mg/ml) in concentrations of 20, 15, 10, 5, 2,5 and 0 µg/ml. The standards were diluted in 0,9% NaCl. 10 µl of each standard dilution was mixed with 2 µl of RIPA Lysis Buffer. 2 µl of the isolated protein samples were mixed with 10 µl of 0,9% NaCl. Standard samples and protein samples were pipetted into a 96-well plate in duplicates. The BCA working reagent was prepared by mixing 50 parts of BCA Reagent A with one part of BCA Reagent B (50:1, Reagent A:B). 0,2 mL of the BCA working reagent was added to each well. Samples were incubated for 30 min at 37°C and absorbance was measured at 562 nm using the Spark ™ 10M multimode microplate reader (TECAN). The protein concentration was calculated by comparing the absorbance of the sample to the absorption coefficient determined from the BCA standard curve.

3.4.3 SDS-PAGE and Western Blot

Proteins were separated by Sodium Dodecyl Sulfate Polyacrylamide (SDS) gel electrophoresis according to their molecular mass. Depending on the protein concentration, 10-30 µg of protein were loaded on NuPAGE ™ Novex ™ 4-12% Bis-Tris Protein Gels (Invitrogen). The gels were rinsed with water and placed in electrophoresis chamber. Electrophoresis tank was filled with 1x running buffer consisting of 25 ml NuPAGE MES SDS Running Buffer (Novex) and 425 ml deionized water. The same amount (in µg) of protein was loaded onto the gels. Therefore, protein samples were diluted in protease-free water (Sigma-Aldrich). 4x NuPage LDS Sample Buffer (Novex) and 10x reducing agent (DTT, 1 M) were added to the diluted protein samples. Samples were heated for 5 min at 95°C to ensure protein denaturation. 5µl of SeeBlue Plus2 Pre-stained Protein Standard was mixed with 5 µl Magic Mark ™ XP Western Protein Standard (Novex), 1:1) and was loaded together with protein samples onto the gel. Electrophoresis was performed at 140 V. Then, proteins were blotted and immobilized onto activated PVDF membranes (BioRad) by using a wet transfer (Trans-Blot Cell, BioRad). 1x Blotting buffer consisting of 40 ml 20x Bolt Transfer Buffer (Novex), 160 ml 20% Methanol and 600 ml deionized water was cooled at 4°C prior use. The SDS-gel was placed on PVDF membrane, which was then sandwiched between filter paper (Whatman Filter Paper, GE Healthcare) and sponges. The transfer case was placed together with an ice-cube box in blotting chamber. Blotting was performed for 1.5 h at 160V and 250 mA. Thereafter, the membrane was stained with Ponceau S solution (Sigma-Aldrich) to confirm successful protein transfer and was blocked for 1 h in TBS-Tween (TBST) containing 5% milk powder. The membrane was incubated with primary antibody at 4°C overnight. After three washing steps with TBST, the membrane was incubated with HRP (Horse radish peroxidase) - linked secondary antibody for 2h at RT. Following the same washing procedure, the membrane was finally washed with TBS. The protein of interest was detected by Pierce ECL Western Blotting Substrate (Thermo Scientific). Detection Reagent 1 and 2 were mixed at a 1:1 ratio and incubated on the blot for 5 min. Chemiluminescence was captured using FluorChem HD2 High Dynamic Range Imaging System (Alpha Innotech). Exposure time was dependent on the intensity of the chemiluminescent signal. The membranes were then stored in TBS at 4°C. All antibodies were diluted in TBST containing 5% milk powder. The used primary and secondary antibodies are listed in table 7. Protein expression was evaluated using Image Studio Lite (LI-COR Bioscience). The bands on the membrane were selected individually to determine signal intensity. Sample signal intensities were then normalized to beta-Actin, which we used as internal loading control.

3.5 Mouse studies and liver sample preparation for electron microscopy

3.5.1 Mouse studies

All mouse experiments were performed at the German Institute for Nutritional Research in accordance with institutional guidelines and approved by the corresponding authorities. Briefly, adenoviruses expressing green fluorescent protein (GFP) and Cre-recombinase (CRE) were generated by Adeno-X Expression System 2 (Clontech Laboratories). P53-floxed mice (C57BL/6 Trp53 ^{tm1Brn}/J) were tail-vein-injected with either adenovirus expressing GFP (control) or CRE (p53 deletion). Three days later, mice were separated again. One cohort of mice that expressed either GFP or CRE was fed *ad libitum*, and another cohort was fasted for 24 h. Mice of both cohorts were sacrificed at the same time. Altogether leading to 4 groups of mice: fasted and fed; acute liver-specific p53 deletion and wildtype.

3.5.2 Electron microscopy

Liver samples were further proceeded for electron microscopy by the Core Facility Ultrastructure Analysis on the Institute for Cell biology, Histology and Embryology Briefly, samples were incubated in 2% paraformaldehyde/ 2.5% glutaraldehyde (PFA/GA) for 3 h and fixed in 0,1 M cacodylat-buffer at 4°C overnight. The following day, samples were post-fixed in 0,2 M cacodylate-buffered 2% osmium solution for 3h. Then, samples were washed in 0,1 M cacodylat-buffer for 3h. After dehydration in an ethanol gradient (50% ethanol [30 min], 70% ethanol [30 min], 80% ethanol [overnight], 96% ethanol [30 min], 100% ethanol [2 x 15 min]), propylenoxide was added for 1h. Samples were impregnated in a 1:1 dilution of propylenoxyd/ TAAB embedding resin (TAAB, UK) and embedded in propylenoxid/TAAB (1:2) overnight. The following day, samples were incubated twice in fresh resin at 45°C and polymerized at 60°C for 3 days. Samples were sectioned and placed onto grids. Finally, grids were stained with 2% uranyl acetate and lead citrate to improve contrast.

3.5.2.1 Sampling

Ultrathin sections were examined in a Tecnai G2 20 electron microscope (FEI, USA), equipped with a Gatan US 1000 digital camera (Gatan, USA). The acquisition of the electron micrographs was supervised by Dr. Andreas Prokesch. The sampling was done unbiased and randomly. 10-15 images were taken from each section to get over 40 images per group. Blind analysis of the samples was done to guarantee an objective quantification.

3.6 Statistical analysis

If not stated otherwise, cell culture experiments were performed at least in triplicates. Statistical analysis was done using GraphPad PRISM 7.0b. Bar graph data were shown as means ± SEM. Significant differences between 2 groups were assessed by two-tailed unpaired one-way ANOVA followed by multiple-testing correction (Tukey's Multiple Comparison Test). Corrected values of $p < 0,05$ were considered as statistically significant in comparison to the respective control.

4 Results and Discussion

4.1 Establishment of a culture model system that reflects hepatic p53 stabilization upon starvation

To further investigate the relation between starvation and p53 signaling, it was aimed to establish an *in vitro* cell culture model and to test whether starvation-induced p53 protein accumulation is cell autonomous. Therefore, cultured hepatocytes were subjected to nutrient-free starvation conditions following western blot analysis and gene expression analysis.

4.1.1 Starvation failed to induce p53 protein levels in AML-12 cells

In the past, Prokesch et al. showed that the p53 protein is stabilized under starvation in mice [42]. To explore the impact of starvation-induced p53 protein accumulation *in vitro*, the murine hepatocyte line alpha mouse liver 12 (AML-12) was tested. This hepatocyte line was derived from livers of mice (CD1 strain, line MT42) transgenic for human transforming growth factor alpha (TGF alpha) and harbor endogenous wild-type p53 [43]. AML-12 cells are continuously replicating and are non-tumorigenic, which makes it a suitable cell line model. Noteworthy, the establishment of AML-12 cells did not require immortalization with SV40, which interferes with p53 expression [44]. However, starvation failed to affect p53 protein levels (**Fig 3).**

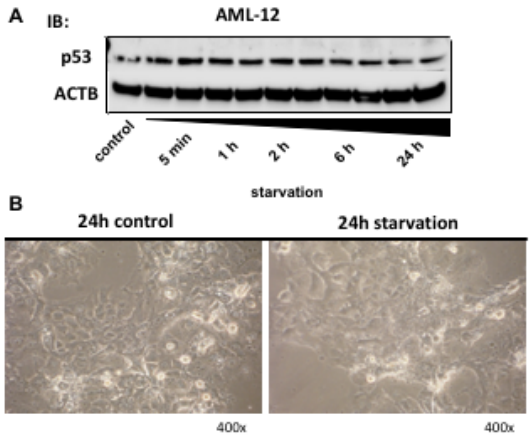

Figure 3: Starvation failed to induce p53 protein levels in AML-12 cells. (A) AML-12 cells were starved in HBSS/HEPES for 24 h. p53 protein levels were detected by Western Blot. ACTB served as internal loading control. (n=1) **(B)** Morphology of AML-12 cells cultured in either growth medium or starvation medium. Morphology was visualized and photographed under a light microscope. Seeding density was 1x 10^5 cells/ml

Fasting induces specific metabolic adaptions and different biochemical pathways become activated to maintain cellular homeostasis [45]. Because p53 signaling is complex and often context specific, it is possible that the p53 protein only plays a minor role in the starvation response in AML-12 cells. Previously, Su et al. demonstrated that the p53 family member and p63 isoform *TAp63* transcriptionally regulate Silent information regulator T1 (Sirt1), AMPKα2, and AMPK-liver kinase B1 (LKB1) in AML-12 cells in response to glucose starvation. Sirt1, AMPKα2, and LKB1 are important metabolic regulators [46]. Sirt1 protein levels is known to increase in response to nutrient deprivation in cultured cells and mice tissues including brain, heart, muscle, and white adipose tissues to maintain glucose and fat homeostasis [47], while AMPK, a key nutrient sensor, become activated through phosphorylation by the tumor suppressor LKB1 in response to energy stress [48]. Su et al

further showed that the transcriptional activation of *Sirt1, AMPKα2, and LKB1* caused an increase in fatty acid synthesis and a decrease in fatty acid oxidation, indicating the role of TAp63 in cellular metabolism [46]. Since the p53 family members p63 and p73 are known to induce many p53 target genes [51], it could be possible that p63, rather than p53, is involved in the regulation of metabolism in AML-12 cells. Moreover, it has been demonstrated that mutant p53 inactivates TAp63 [52], indicating an interplay between p53 family members in the regulation of cellular metabolism in cancer [46]. Hence, the role of different p53 family members in the starvation response in AML-12 cells needs to be clarified.

4.1.2 Stabilization of p53 protein under starvation in primary human hepatocytes

To assess whether hepatic p53 is stabilized upon starvation in humans, primary human hepatocytes of two different healthy donors were starved for 24 h.

Consistent with the previous findings of Prokesch et al. in fasted mice (**Fig 2 A, B** [42]) p53 protein levels accumulated after 24h of starvation in primary human hepatocytes (**Fig 4 A**). Additionally, p53 mRNA expression was not affected by starvation (**Fig 4 B**), indicating that this effect was likely mediated by posttranscriptional p53 stabilization.

Primary culture of adult human hepatocytes has become the gold standard model to assess human relevant metabolism studies. However, the shortage of human liver samples of adequate quality and difficulties with long-term maintenance of liver cells with high viability and liver-specific functions remain a major challenge. It has therefore become mandatory to develop alternative sources of human hepatocytes [53].

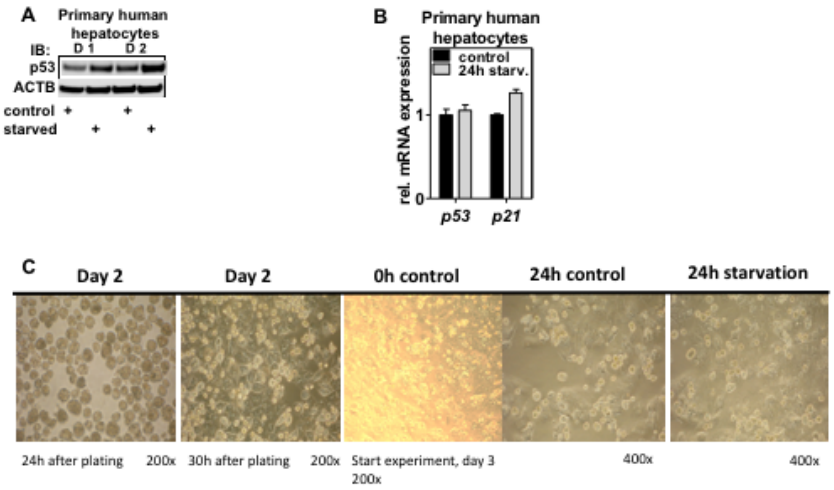

Figure 4: Stabilization of p53 protein under starvation in primary human hepatocytes. (A) Primary human hepatocytes were starved in HBSS/HEPES for 24 h and p53 protein levels were detected by Western Blot. ß-Actin was used as loading control. (n=2) **(B)** qPRC analysis of p53 mRNA expression after 24h starvation (n=2) **(C)** Morphology of primary human hepatocytes cultured in either growth medium or starvation medium. Morphology was visualized and photographed under a light microscope. Seeding density was 0,8x 10^6 cells/ml

4.1.3 Changes of p53 protein levels under starvation in HepaRG cells

The recent development of the human hepatoma cell line named HepaRG has shown immense potential as an *in vitro* system to investigate the molecular pathways in human hepatocytes [53, 54]. Previous studies in HepaRG cells have demonstrated that p53 protein levels are detectable and accumulate in response to DNA damage. Sequencing of *TP53* confirmed the presence of wild-type sequence [55].

To test if this cell line could be an alternative to cultivated primary human hepatocytes in our settings, differentiated HepaRG cells were subjected to starvation medium for 24h. Indeed, starvation resulted in an induction of p53 protein levels **(Fig 5 A).** However, qPCR analysis revealed an increase in p53 mRNA expression after 24h of starvation. Thus, the observed accumulation of p53 protein could be due at least partly to increased p53 mRNA expression. In contrast, mRNA levels of cyclin-dependent kinase inhibitor 1A (*Cdkn1a* or *p21*), a target gene of p53, did not changed upon starvation.

HepaRG cells are human bipotent progenitor cells, which are able to differentiate toward two cell types, biliary-like and hepatocyte-like cells [56]. HepaRG cells proliferate until they reach confluence and differentiate into fully developed hepatocyte-like cells when culture medium is supplied with 2% Dimethylsulfoxide (DMSO) and hydrocortisone [57]. Once committed, they differentiate into hepatocyte-like and primitive biliary cells, mostly resulting in a 1:1 ratio [58]. Although primitive biliary cells are not well characterized, the manufactures suggested that they contribute to the long-term maintenance of HepaRG through communication with differentiated hepatocyte-like cells [59, 60]. Previously, it has been shown that the differentiation status of HepaRG was only reached after a prolonged quiescence and when the cells were maintained at confluence associated with a DMSO treatment. Further, DMSO treatment was necessary for a high-level expression of cytochrome P450 and the susceptibility of HepaRG cells to hepatitis B infection [57]. In addition, Cerec et al. proposed that the survival and proliferation of differentiated HepaRG cells depends on the apoptotic regulators p53, and CDK-inhibitors p21 and p27. They demonstrated that p53 protein and RNA expression were constant during the differentiation process and dropped in DMSO-treated culture, which correlated with growth arrest and differentiation. Moreover, p21 protein expression transiently increase during the proliferation phase and strongly decrease in differentiated cells, which support low apoptotic activity and high proliferation potential of differentiated cells [55 and 61]. Thus, DMSO treatment is required for fully metabolic activity of HepaRG cells [57] and a decrease in p53 expression is associated with differentiation [61]. However, the mechanism in which DMSO increase some liver-specific functions in HepaRG cells is still not known. Another study showed that DMSO functions as a reactive oxygen species scavenger and an anti-apoptotic agent in primary rat hepatocytes [62]. Thus, changing culture medium to starvation medium without DMSO could re-introduce p53 expression, leading to the observed increase in p53 mRNA expression. Paradoxically, another study showed that differentiation of HepaRG cells is associated with the downregulation of the Akt-mTOR pathway. Since mTOR is a critical component of translational control, they analyzed polysome-bound transcripts and demonstrated that enhanced activity of mTOR specifically impaired the up-regulation of genes including members of the TNF/caspase transduction pathway and transcription factors associated with lipid homeostasis, preventing hepatocytic differentiation [63]. However, these findings disagree with the previous described downregulation of p53 protein upon DMSO-treatment because p53 is a well-known negative regulator of the AKT/mTOR pathway [64]. Thus, further characterization of differentiated HepaRG cells need to be done before HepaRG can be used as suitable cell line for investigating p53 signaling upon starvation.

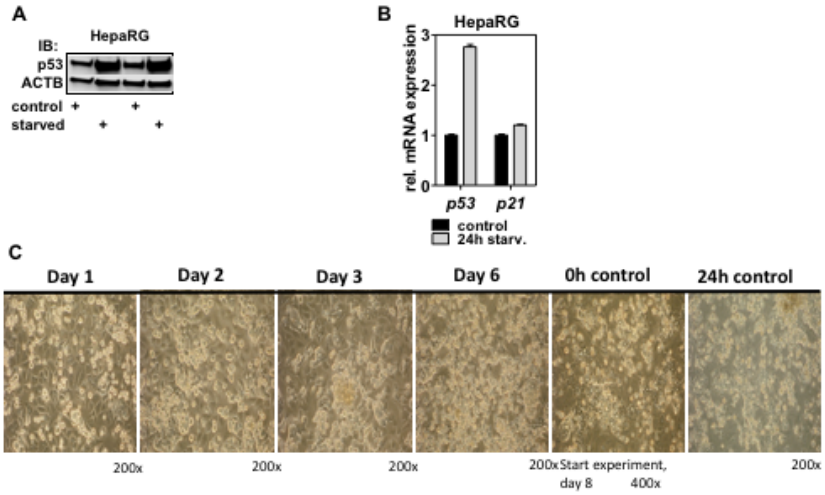

Figure 5: p53 protein is stabilized by starvation in HepaRG cells. (A) Hepatocytes were starved in starvation medium for 24h. Western Blot analysis were performed to determine p53 protein levels and ACTB served as loading control **(B)** qPCR analysis of p53 and p21 mRNA expression after 24h of starvation. Expression levels are set to 1 in control (n=2) **(C)** Morphology of HepaRG cells cultured in either growth medium or starvation medium. Morphology was visualized and photographed under a light microscope. Seeding density was 1x 10^6 cells/ml

4.1.4 Upcyte hepatozytes as an alternative cell line model

Because starvation experiments in the HepaRG cell line failed to reproduce the *in vivo* scenario, a second alternative to primary human hepatocytes was tested. Upcyte hepatocytes are expanded functional human hepatocytes derived from a single donor, which exhibit primary cell morphology and polarity. To expand human hepatocytes, upcyte hepatocytes were stimulated with growth factors to express the human papilloma virus (HPV) oncogenes *E6* and *E7*. The E7 protein expression prevents the transition from G1 to S phase, inducing proliferation. The E6 protein expression inhibits p53 tumor suppressor's function to induce cell cycle arrest. Thus, the expression of E6 and E7 were associated with cell-cycle arrest without immortalization. Furthermore, the expression of E6 and E7 upregulates the expression of the oncostatin M (OSM) receptor gp130. Treatment with OSM allows the isolation of cell colonies, which express E6 and E7 at low levels. Removal of OSM then induced the differentiation of the cells into hepatocytes with transcriptional, metabolic and toxicity profiles similar to those of primary human hepatocytes [65, 66].

Although Upcyte hepatocytes expressed E6 at low levels [65], E6 expression did not interfere with basal p53 expression under normal conditions. Treatment with the p53 activator Nutlin-3a further increased the p53 protein levels. Nutlin-3a was reported to induce p53 accumulation by inhibiting its interaction with its negative regulator Mdm2 [67]. Thus, p53 is present and inducible in Upcyte hepatocytes **(Fig 6 A).** However, starvation conditions failed to induce p53 stabilization. Since starvation is a prominent trigger for autophagy, autophagic flux was also measured [68]. Treatment with Bafilomycin, an autophagy inhibitor [69] increased the lipidated version of microtubule-associated protein light chain 3 (LC3-II) at the beginning of the experiment (0h), which indicates functional basal autophagy activity [70]. However, a 24 h cultivation in either normal medium or starvation medium strongly diminished LC3 protein levels, while 48h of cultivation with and without Bafilomycin treatment resulted in accumulation of LC3 protein levels **(Fig 6 B).**

The seemingly reduction of protein levels under starvation conditions can be attributed to dissimilar loading. But, Ponceau staining of the membrane revealed an equal loading of the gels. Reversible Ponceau staining is validated as an alternative to actin blotting [71].

Previous studies of Prokesch et al have already shown that starvation-induced accumulation of p53 protein in primary hepatocytes and HepG2 cells was due to AMPK activation [42]. However, treatment with the AMPK activator AICAR [72] had no effect on p53 protein expression. Taken together, these findings indicate that Upcyte Hepatocytes did not serve as suitable cell line model to investigate p53 stabilization upon nutrient deprivation.

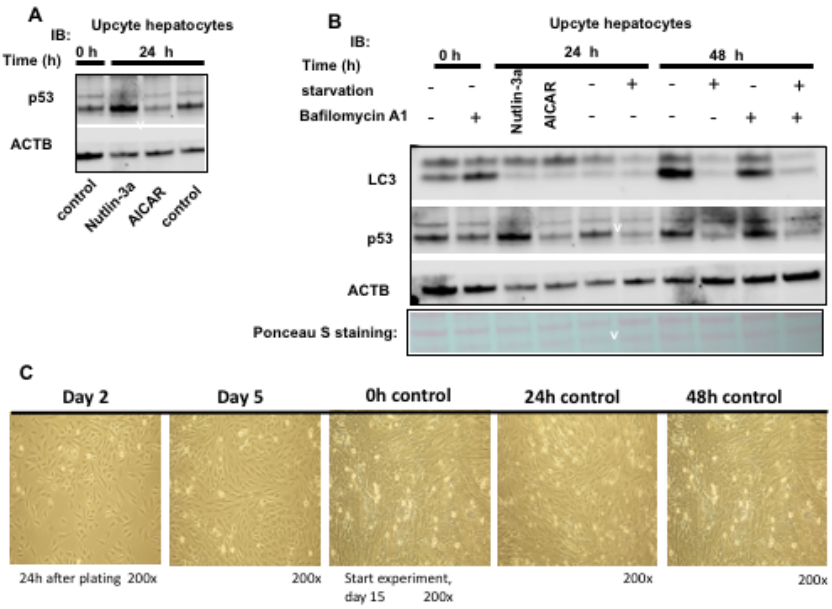

Figure 6: upcyte hepatocytes as an alternative cell line model. (A) Hepatocytes were treated for 24h with 10 µM nutlin-3a, 0,5 mM AICAR, or with DMSO as vehicle control and analyzed for p53 expression (n=1). **(B)** Upcyte Hepatocytes were starved for 24h and 48h and treated with 10 nM Bafilomycin A or DMSO as vehicle control and Western blot analysis was performed to determine LC3-II protein levels. Equal loading was confirmed by Ponceau S staining. **(C)** Morphology of Upcyte Hepatocytes cultured in either growth medium or starvation medium. Morphology was visualized and photographed under a light microscope. Seeding density was 1x 10^6 cells/ml

4.1.5 Stabilization of p53 protein levels in HepG2 cells

The human hepatoma cell line HepG2 is routinely used for hepatocyte-specific studies. Although these cells are not hepatocytes *per se,* because of their dedifferentiated and abnormal hepatic phenotype, HepG2 cells represent a very useful tool for basic research [53]. Furthermore, HepG2 cells express a non-mutated wildtype *p53* gene [73].

Starvation of HepG2 cells resulted in a time-dependent induction of p53 protein and significantly increased after 48h of starvation. **(Fig 7 A**). Gene expression analysis revealed that p53 mRNA levels did not significantly increase upon starvation, suggesting that the p53 accumulation corresponds to post-translational stabilization in response to starvation **(Fig 7 B).** This supports the previous findings (**Fig 2 A, B,** [42]) Moreover, 48h of starvation did not affect the cell morphology **(Fig 7 C).** Therefore, the experimental studies were performed using the HepG2 cell line.

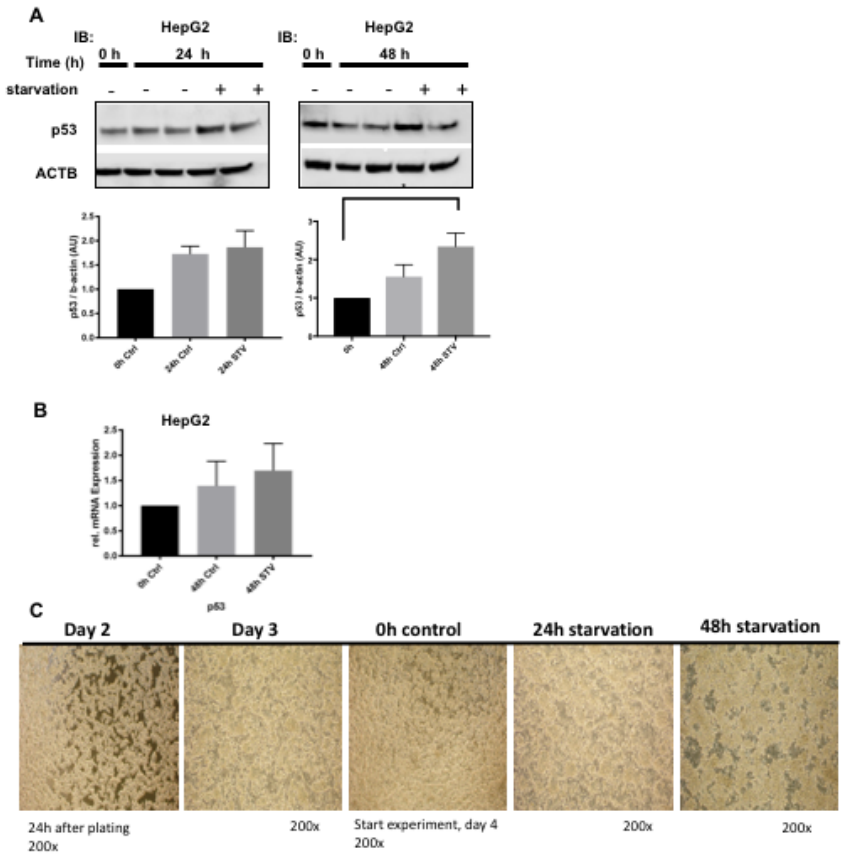

Figure 7: stabilization of p53 protein levels under starvation in HepG2 cells. HepG2 cells were starved in HBSS/HEPES for 24 h or 48 h. (**A)** Western Blot analysis was performed to determine p53 levels and ACTB served as loading control (n=3). Protein expression levels were set to 1 in control (0h) (**B)** qPCR analysis of p53 mRNA expression after 48h starvation. Expression levels were normalized to GAPDH as internal control (n=3) (**C)** Morphology of HepG2 cells cultured in either growth medium or starvation medium. Morphology was visualized and photographed under a light microscope. Seeding density was $1x10^6$ cells/ml

4.2 P53 protein stabilized despite the general decline in total protein content under starvation in HepG2 cells

To monitor starvation-induced protein dynamics in HepG2, cells were incubated in starvation medium for indicated times. Routinely, the total protein concentration of samples for Western Blot analysis were determined by the Bicinchoninic acid (BCA) assays [75]. Strikingly, we recognized that the total concentration of protein measured by BCA decreased upon starvation (**Fig 8 A).** Hence, equal amounts of cell lysates were separated by SDS-PAGE and blotted on membranes to investigate the degradation of proteins in a time-dependent manner. Ponceau S staining of the blotted protein samples showed a subtle, time-dependent decrease in the cellular protein content **(Fig 8 B).** This effect could be related to bulk degradation of long-lived proteins. Thus, the membrane was further incubated with anti- ß Actin antibody, since ß-Actin (ACTB) is a known stable protein with long half-live [74]. Indeed, a decline in ACTB protein levels could be detected (**Fig 8 C).** Nutrient deprivation is a powerful inducer of autophagy [76], which is thought to be responsible for cytoplasmic bulk degradation and therefore for turnover of long lived proteins [77]. LC3 is a widely-used marker of autophagosomes in mammalian cells [27] and the turnover of LC3 indicates autophagic flux [78]. Strikingly, LC3 protein did decrease after nutrient deprivation **(Fig 8 C).** However, these findings need to be interpreted with caution because LC3 levels can vary in response to different stresses. Thus, accurate detection of autophagy requires the performance of "autophagic flux assays" [68, 70, 78]. Next, the activity of mTORC1, a major inhibitor of autophagy [79], was observed. The ribosomal protein S6 kinase 1 (P70S6K1) is a downstream target of mTORC1. Phosphorylation by mTORC1 stimulates p70S6K activity and leads to increases in mRNA biogenesis, cap-dependent translation and elongation, and the translation of ribosomal proteins [80]. As expected, P70S6K1 activity diminished upon starvation (Fig 8D), suggesting mTORC1 inactivation and consequently autophagy induction [81]. In contrast to the general trend of protein degradation after nutrient deprivation, p53 protein levels increased starting with 4 hours and stabilized after 8 – 24 hours of starvation **(Fig 8 C).** It is therefore tempting to speculate that p53 is important to survive periods of starvation and that the loss of p53 would additionally threaten cellular survival [42, 82].

In agreement with these results, Kristensen et al. showed that autophagy is the main pathway for starvation-induced protein degradation in MCF7 cells [77]. Furthermore, quantitative mass spectrometry of MCF7 cells under starvation conditions revealed a strong degradation of proteins involved in translation, such as ribosomal protein S6, while nuclear proteins or vacuolar proteins involved in degradation processes remained constant, indicating their importance during amino acid starvation. Thus, the authors hypothesized that autophagy is a selective rather than an unspecific process [77]. Indeed, there is increasing evidence that macroautophagy specifically recognize their cargo by cargo-recognition molecules or autophagy receptors [83, 84]. This specificity is believed to be important for cellular survival during conditions of nutrient deprivation and basal autophagy. During starvation, selective degradation of non-essential proteins provides amino acids that can be used to sustain synthesis of proteins required for survival [85]. In line with these findings, another recent study demonstrated that p53 has a central role in the regulation of autophagy and that nutrient deprivation, as a form of cellular stress, activates nuclear p53, promoting autophagy induction [86]. Furthermore, it has been shown that p53 by itself is not a direct target of autophagy degradation [87], which confirms our hypothesis that p53 stabilization is required for adaption of metabolism possible by selective protection from autophagy degradation [42]. Thus, p53 stabilization by fasting could have also implications in autophagy regulation in HepG2 cells. Another explanation for the observed increase of p53 protein levels could be that starvation induced the degradation of its negative regulator Mdm2. Previous studies have shown that hispolon, a chemotherapeutic agent, induced Mdm2 downregulation through the CMA pathway

[49]. However, further studies are needed to investigate whether Mdm2 is degraded through macroautophagy upon starvation. Taken together, this experiment support the idea that starvation induces the bulk degradation of long-lived proteins, possibly due to autophagy. Therefore, experiments to examine the correlation between p53 accumulation and autophagy in HepG2 were performed next.

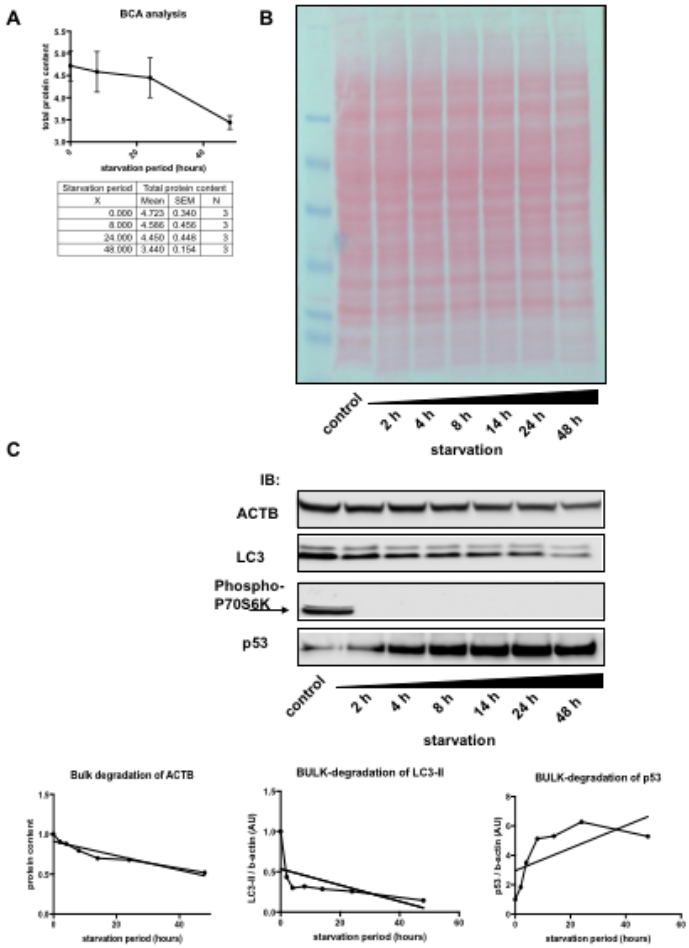

Figure 8: Bulk degradation of long-lived proteins after starvation. Decline in total protein content after nutrient deprivation of HepG2 cells**.** HepG2 were starved for indicated times **(A)** 20 µl of HepG2 cell lysates were separated by SDS-Page and blotted onto nitrocellulose membrane. The membrane was stained with Ponceau S dye**. (B)** Total protein content was determined with a bicinchoninic acid assay (BCA). Quantification of total protein content (means ± SEM, n=3**). (C)** Western Blot analysis of ß-Actin, LC3**,** p-P70-S6K (Thr389), and p53 after 0-48 h of starvation. Graphs represent the decline in protein content. Expression of ACTB served as loading control (n=1).

4.3 Monitoring Autophagy in starved HepG2 cells

Accumulating evidence indicates that p53 can regulate autophagy depending on its subcellular localization [40, 86, 88]. It has been shown that cytoplasmic p53 suppress autophagy [89], while nuclear p53 induce autophagy [90]. To investigate the impact of p53 on autophagy in HepG2 cells, the autophagic flux was monitored. The term "autophagic flux" refers to the dynamic process of autophagosome synthesis, fusion of the autophagosomes with a lysosome, and degradation of autophagic substrates inside the lysosome [70]. Endogenous LC3-II, a specific marker of autophagosomes, is widely used to measure autophagic flux. Upon autophagy induction, the lipidated form of LC3 (LC3-II) binds to the inner and outer membrane of autophagosomes and is degraded after fusion with lysosome [91]. However, it is very important to notice that increasing numbers of autophagosomes in a cell, observed by increased LC3-II protein levels, does not always correspond to increased cellular autophagic activity. The number of autophagosomes is regulated by both the rate of their generation and their conversion into autolysosomes at a given time point. Consequently, accumulation of autophagosomes could be either due to increased autophagy induction or due to a blockage of autophagosome degradation [92]. To distinguish between these two possibilities, it is necessary to monitor the degradation of endogenous LC3 in presence and absence of lysosomal inhibitors (LC3 turnover assay) [70]. It has been well demonstrated that Bafilomycin A1, a macrolide antibiotic, inhibits the vacuolar-type H (+)-ATPase, thereby increasing the intralysosomal pH by preventing the transition of protons into the lysosomal lumen. Thus, acidification of lysosomes and endosomes is inhibited [69, 93]. It has been further shown that, in addition to the inhibition lysosomal acidification and lysosomal enzyme activation, Bafilomycin A1 also targets other types of ATPases, which cause a block in autophagosome-lysosome fusion [69]. Consequently, autophagic flux degradation is inhibited, resulting in the accumulation of the autophagy marker LC3-II. Hence, the differences between LC3-II levels in presence and absence of the inhibitor represents the autophagic flux (**Fig 9 A**) [94].

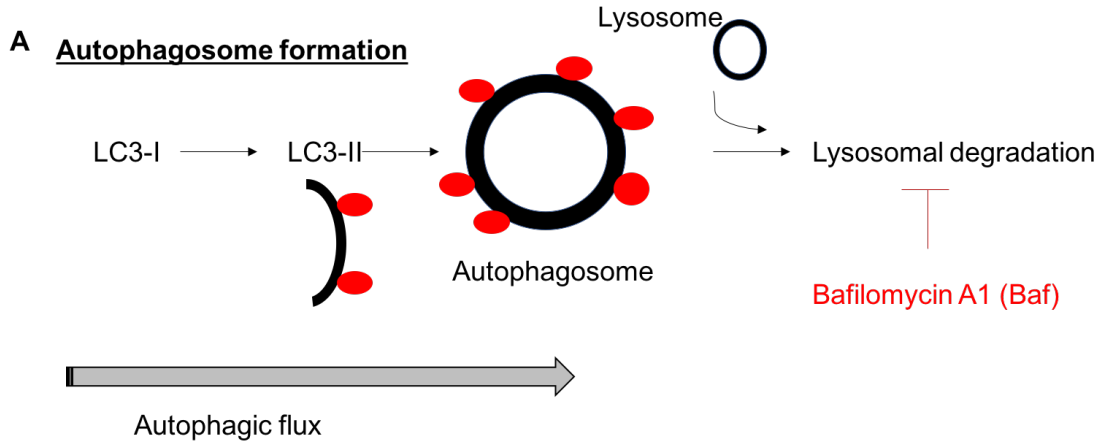

Figure 9: Monitoring Autophagy in starved HepG2. (A) Schematic description of autophagic flux. Cytosolic LC3-I conjugate to phosphatidylethanolamine (PE) to generate LC3-II, which is important for the formation of autophagosomes. Subsequently, autophagosomes fusion with lysosome, leading to LC3-II degradation. Treatment with Bafilomycin A1 blocks the late maturation steps. Adopted from Metz et al. [95]

4.3.1 Nutrient deprivation induces autophagy in HepG2 cells

As mentioned in the previous paragraph, it is crucial to measure LC3-II protein levels in presence and absence of autophagy inhibitors for every experimental condition to assess autophagic activity [96, 97]. Autophagy exists constitutively in all eukaryotic cells to maintain cellular homeostasis (basal autophagic flux) and can be activated in response to various stimuli (induced autophagy) [98]. Noteworthy, it has been reported that the degree of basal autophagy, as well as the capacity to induce autophagy in response to stress, varies in different mammalian

cell lines and tissues [96, 99]. Moreover, autophagy induction in cultured cell lines varies between different autophagy inducers. For instance, cultivation of cells in Earle's Balanced Salt solution (EBSS), which lacks essential amino acids, increased the autophagic flux within 2 hours, while serum starvation induced autophagy after 12-24h of cultivation. Noteworthy, most cells undergo cell death after incubation with EBSS for more than 4-8 h [96]. Hence, it is recommended to test autophagic flux at early and late time-points, to characterize autophagy modulators [78]. Thus, autophagic activity was monitored at different time points in HepG2 cells to investigate its capacity, when exposed to nutrient deprivation [78]. HepG2 cells were cultured in either nutrient-free medium or normal culture medium and treated with 10 nM Bafilomycin A1 for the last 2 hours of incubation. DMSO was used as control. Protein samples were harvest and analyzed by Western blot for LC3B. Notably, anti-LC3B antibody detects LC3-I and LC3-II, which can be distinguished based on their different electrophoretic mobility [68]. Lipidated LC3-II migrates faster than LC3-I, most likely due to its hydrophobicity. LC3-II bands are usually detected on a gel at a molecular mass around 14 kD [31].

As seen in **Fig 10 A**, LC3-II strongly accumulated in the non-starved samples (control) and slightly increased in the presence of Bafilomycin A1, indicating basal autophagic flux in HepG2 cells after 8h of cultivation [78, 100]. However, the LC3-II levels did not further increase in the presence and absence of Bafilomycin A after 8h of starvation (**Fig 10 A**). Hence, these findings indicate that 8h of starvation did not induce autophagic flux in HepG2 cells [70 ,97]. The data was consistent with findings obtained in HepG2 cells, cultured in low glucose conditions **(Fig S1).** Although 8h of starvation did not further induce autophagy, this result cannot be interpreted as "steady state". To measure the steady-state of autophagy, time-lapse analysis of LC3-II levels would be required without any fusion inhibition [101]. Strikingly, LC3-II levels were highly induced after 24 h and 48 h of starvation, indicating an increase in autophgic flux [78]. **(Fig. 10 A)**. Importantly, monitoring autophagic flux via LC3-II turnover at a given time point does not absolutely measure a flux per se, although the use of autophagic inhibitors is largely accepted to interpret results on LC3-II immunoblotting [78]. Thus, LC3-II signal should be monitored over time during the Bafilomycin A1 treatment to estimate the autophagic rate. Indeed, autophagic flux, calculated by dividing the value of LC3-II in presence of Bafilomycin A by that in absence of Bafilomycin A [41], was increased upon starvation over time **(Fig 10 B).** Taken together, autophagy was induced during prolonged starvation conditions in HepG2 cells.

4.3.2 Possible correlation between p53 stabilization and autophagy induction upon prolonged starvation in HepG2 cells

As shown in **Fig. 10 B**, autophagic flux was significantly induced after 48h of starvation. Moreover, prolonged starvation induced the accumulation of p53 protein with a significant increase in p53 levels after 48h starvation **(Fig 10 A**). As mentioned before, p53 was shown to act upstream of the autophagy pathway [15, 40, 84]. As expected, p53 protein levels did not differ significantly in presence and absence of Bafilomycin after 24h in normal or starvation medium. However, statistical analysis revealed a significantly decline in p53 protein levels after 48h of starvation upon Bafilomycin treatment **(Fig 10 A).** Thus, Bafilomycin treatment may contribute to the decrease in p53.

One explanation for the decreased p53 protein level upon Bafilomycin treatment could be that inhibition of macroautophagy triggers apoptosis [102] Boya et al., demonstrated that mammalian cells underwent apoptosis under conditions of starvation and simultaneous inhibition of macroautophagy either genetically or pharmacologically. They showed that treatment with Bafilomycin A1 caused the expected accumulation of LC3-II in normal and starvation conditions. However, while starvation alone did not cause major cell death, apoptosis

was induced when Bafilomycin A1 was added to starved cells. Cell death most likely occurred through mitochondrial membrane permeabilization (MOMP). [103]. In agreement with these results, it has been shown that cytoplasmic p53 can directly target mitochondria for cell death induction [104]. Marchenko et al. showed, that a fraction of stress-stabilized p53 transfer to mitochondria to induce p53-dependent apoptosis in fast kinetics. They further demonstrated that cellular p53 translocated to the mitochondria within 30-60 min after the initial stress stimulus and prior to detectable nuclear accumulation in hematopoietic cells [105]. At the mitochondrion, p53 triggered MOMP, thereby inducing apoptosis most likely due to protein-protein interactions with Bcl-2 family members, such as Bcl-2, Bax or Bak [88]. Thus, it is tempting to speculate, that starvation and autophagy inhibition by Bafilomycin A triggers rapid translocation of p53 to mitochondria and induce mitochondrial-mediated cell death. Hence, the rapid transfer of p53 to mitochondria could explain the observed decrease in p53 protein levels on Western Blot. However, according to Marchenko et al. only a small fraction of stress-induced p53 translocated to mitochondria and p53 protein levels was still detectable in Western Blot analysis of whole cell lysates [105]. Moreover, RIPA buffer was used for protein harvest, which can extract membrane-bound, nuclear and mitochondrial proteins, as well as whole cell proteins [106]. Hence, the lysis procedure was not responsible for the decrease in p53 protein levels upon Bafilomycin A treatment and starvation. Thus, to test whether and to what extent p53 translocate to mitochondria in the Bafilomycin treated and starved cells, classical cell fractionation and immune-fluorescence-activated cell sorter analysis needed to be done. In contrast, another study showed that inhibition of autophagy by Bafilomycin A1 induced cell cycle arrest and apoptosis in colon cancer cells, which was accompanied with the up-regulation of *p21Cip1* [107], which is a major transcriptional target of p53 [108]. Consequently, apoptosis assays need to be done to investigate the link between autophagy inhibition, starvation and p53 signaling. However, inhibition of autophagy by Bafilomycin A led to the expected accumulation of LC3-II levels in comparison to untreated cells**.** Consequently, treatment of Bafilomycin A sufficiently inhibited autophagosomal degradation. Thus, pharmacological inhibition of autophagy worked in HepG2 cells. Since 48h of starvation significantly induced p53 stabilization and LC3 accumulation, the following experiments were focused on the 48h time point.

4.4 p53-dependent effects on autophagic flux in HepG2 cells

Previous evidence indicates that p53 can either induce or inhibit autophagy [40, 86, 89]. To further investigate the role of p53 stabilization on autophagy in HepG2 cells, wild-type p53 HepG2 cells (p53 +/+) and p53-depleted HepG2 cells (p53 -/-) were compared. HepG2 p53 -/- cells are isogenic derivate of HepG2, in which the p53 alleles have been knocked out by using the CRISPR-Cas9 system. Efficient p53 knockdown was confirmed by qPCR **(Fig S2)** Surprisingly, the knockout of p53 seemed to affect cell growth. Wildtype HepG2 cells tended to grow in clusters [109, 110], while HepG2 p53-/- cells grew slower and displayed a more enhanced cluster formation **(Fig S2 B).** The reason for the changes in cell growth are not known. However, cell viability was not affected, which was checked routinely by light microscopy (**Fig S2 B**). For nutrient deprivation, cells were subjected to starvation medium for indicated times. Although LC3-I (18 kDa) and LC3-II (16 kDa) bands were seen in both cell types (exposure time about 1 min), band intensity of LC3 were stronger in the p53 -/- cells **(Fig 10 C).** Increased LC3-II levels can be either due to enhanced autophagic activity or reduced autophagosome degradation [68]. To distinguish between these possibilities, Bafilomycin A, an autophagy inhibitior [69], was added 2h prior to protein harvest. Both cell lines displayed autophagosome flux, evident as accumulation of LC3-II in the presence of Bafilomycin A [78, 96, 97]. However, while p53 +/+ HepG2 cells showed a robust, significant increase of LC3-II in presence of Bafilomycin A. LC3-II protein levels only slightly increase in p53 -/- cells (**Fig 10 D**). Additionally, monitoring of the autophagic flux over time revealed a decrease in autophagic

activity in p53 -/- cells in comparison to p53 +/+ cells **(Fig 10 E)**. Hence, autophagy seemed to be defective in absence of p53. Thus, blockage in autophagic flux in p53 -/- cells could have caused the strong LC3-II protein bands [41]. Taken together, we found that p53 deletion is associated with defective autophagy upon prolonged starvation in HepG2 cells.

Previous, Scherz-Shouval et al. demonstrated that p53 loss in starved HCT116 cancer cells caused a decrease in autophagic flux, most likely due to blockage of autophagosome degradation. In agreement to our results, basal LC3-II protein levels accumulated in p53 knockout cells but did not further increase with Bafilyomicn A1 treatment upon prolonged starvation, indicating aberrant autophagosome accumulation [41]. Contrarily, Tasdemir et al. showed, that the knockdown of p53 and pharmacological inhibition with pifithrin-α, a p53 inhibitor, induced autophagy in HCT116 cells and that p53 inhibition even increased autophagic flux in Hela cells [89]. One explanation for these contrary findings could be that p53 regulate autophagy ambiguously, depending on its subcellular localization [40]. Indeed, Tasdemir et al. suggested that cytoplasmic p53 was responsible for autophagy regulation in HTC116 cells [89]. However, another recent study in MEF cells showed that treatment with etoposide, which induces double-stranded DNA breaks and activates p53, induced an increase in LC3-II protein levels in WT MEF cells, whereas little or no increase of LC3-II was observed in p53 -/- cells, suggesting that activation of p53 on autophagy might contribute to its tumor suppressor functions [112]. Although they did not mention whether nuclear or cytosolic p53 was responsible for these findings, it is tempting to speculate, that nuclear p53 was associated with autophagy induction, since they used etoposide as p53 inducer. Hence, further studies, like fractionation assays, need to be done to clarify whether nuclear or cytoplasmic p53 influences autophagy in HepG2 cells. Furthermore, it would be of interest if p53 knock down with a specific short interfering (si) RNA or pharmacological inhibition with cyclic pifithrin-α (PFT-α) mirror the observed reduction in autophagic flux in HepG2

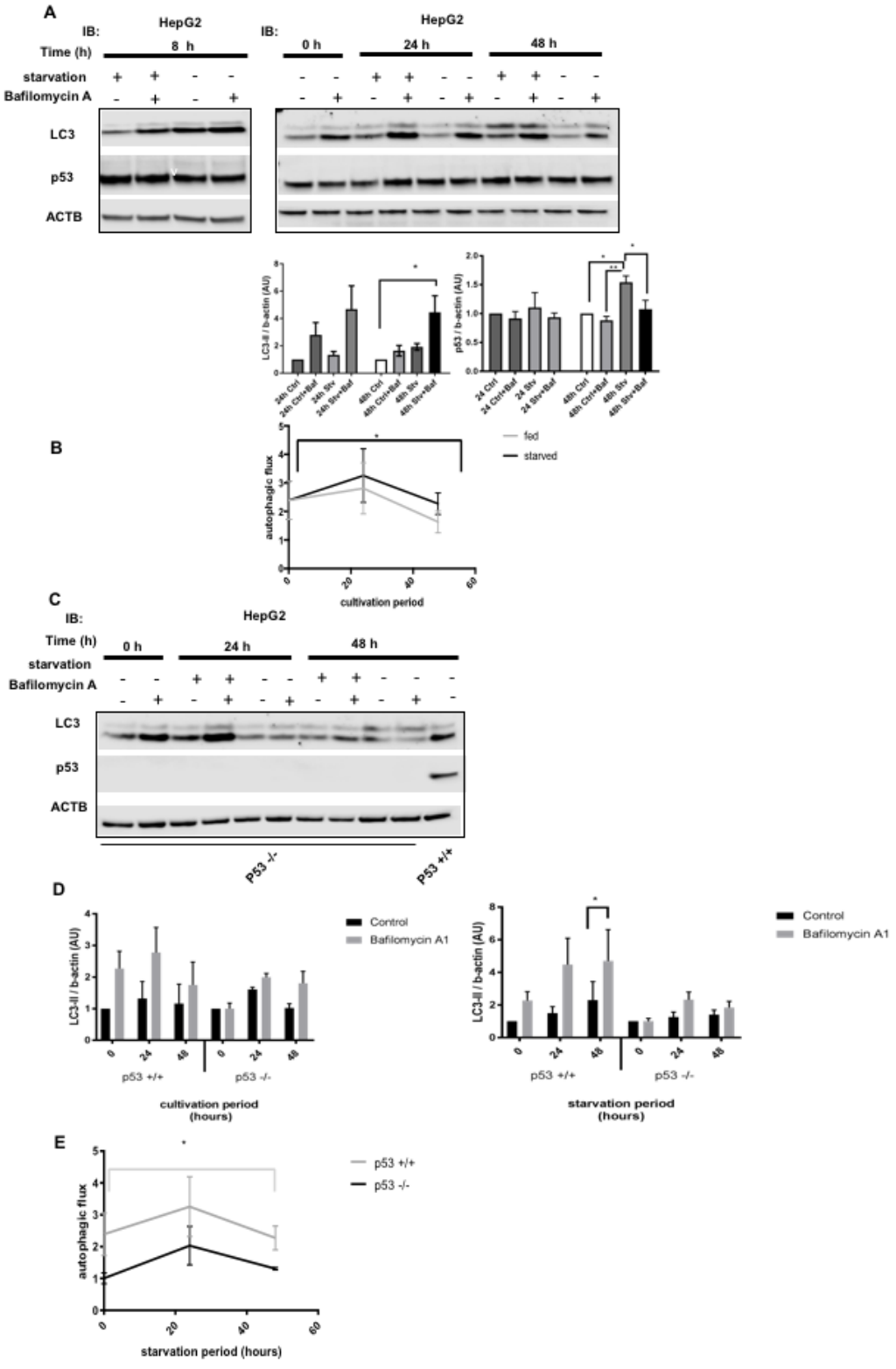

Figure 10: Monitoring Autophagy in starved HepG2. P53 +/+ and p53 -/- cells were subjected to starvation medium for 48h and treated with 10 nM Bafilomycin A1 or DMSO as vehicle control. Treatments were added 2h prior harvest. Protein samples were collected at indicated time points **(A)** Western blot analysis of p53, LC3 and ACTB in HepG2 p53 +/+ cells treated with 10 nM Bafilomycin A1 or DMSO as vehicle control after 8h of cultivation or 48h. ACTB served as loading controls. **(B)** Autophagic flux in HepG2 p53 +/+ cells was calculated by dividing the amount of LC3-II in presence of Bafilomycin by that without Bafilomycin [41] in either starvation medium or high glucose medium. 0h control sample was set to 1 (n=3). **(C)** Western blot analysis of p53, LC3 and ACTB in p53 -/- cells treated with 10 nM Bafilomycin A1 or DMSO as vehicle control. ACTB served as loading controls (n=3) **(D)** Quantification of LC3-II protein

levels in p53 +/+ and p53 -/- cells treated with either Bafilomycin or DMSO. **(E)** Autophagic flux in p53 +/+ and p53 -/- cells was calculated by dividing the amount of LC3-II in presence of Bafilomycin by that without Bafilomycin [41] in either starvation medium or high glucose medium. 0h control sample was set to 1 (n=3).

4.4.1 MAP1LC3 expression is increased in p53 -/- cells

As shown in **Fig. 10 D**, basal LC3-II protein levels were increased in p53 -/- cells in comparison to p53 +/+ cells. To further investigate this difference, LC3 mRNA levels were monitored in p53 +/+ and p53 -/- cells. Gene expression analysis of *MAP1LC3* revealed that LC3 mRNA was significantly downregulated to basal level after 48h of starvation, but was increased after 48h in growth medium in p53 +/+ cells. In p53 -/- cells, LC3 mRNA levels also decreased after 48h of starvation, however, the decrease was not significant. Furthermore, LC3 mRNA expression in p53 -/- cells was higher than in p53 +/+ cells. This effect was seen in basal expression and after 48h of cultivation **(Fig 11 A).** Hence, it is tempting to speculate that p53 is required for downregulation of *MAP1LC3* in long-term starved HepG2 cells.

In agreement with our results, Scherz-Shouval et al showed that p53 knockout in HTC116 cells caused an increase in LC3B mRNA levels in comparison to p53 wildtype cells after 48h of starvation. They further suggested, that cytosolic p53 promotes the degradation of LC3 mRNA on prolonged nutrient deprivation [41]. In contrast, He at al. reported, that LC3 transcription increased in yeast and certain mammalian cells in response to stress, which might induce autophagy [114]. However, the correlation between autophagy induction and transcriptional regulation of autophagy-related genes is still under debate. Moreover, most *ATG* genes, including *MAP1LC3*, and ATG protein levels are cell type- and tissue-dependent. Thus, ATG mRNA and protein expression levels are not recommended for monitoring autophagy [70, 78]. Further, various ATG proteins undergo post-translational modification, which seemed to be more crucial for the regulation of autophagy activity [113] than the regulation of their gene expression [70]. Thus, it is not clear if the observed changes in LC3 gene expression were related to p53 signaling.

4.5 P53 as transcriptional regulator of autophagy-associated genes?

Growing evidence suggests that p53 can induce autophagy by controlling mTOR activity or by direct regulation of autophagy-associated genes [115]. Previous studies have shown that p53 induces AMPK β1, TSC2, PTEN and IGF-BP3 gene expression, which in turn negatively regulates the IGF-1/AKT and mTOR pathways in response to cellular stress [116]. To investigate the impact of p53 as transcription factor of autophagy-associated genes in HepG2 cells, gene expression analysis of tuberous sclerosis complex 2 (TSC2), and damage-regulated autophagy modulator (DRAM) were performed.

The mTOR pathway is one of the best characterized inhibitor of mammalian autophagy. mTOR is a serine/threonine kinase that acts as a key regulator of cellular metabolism and promotes cell growth in response to nutrient and energy availability. It consists of two distinct signaling complexes, mTOR complex 1 (mTORC1) and mTORC2. It has been shown that mTORC1 regulates autophagy, while mTORC2 is not a direct regulator of autophagy [117, 118, 119]. mTORC1 is activated through the small GTPase Rheb in nutrient-rich conditions, while nutrient-poor conditions block mTORC1 signaling through several mechanisms such as AMPK activity. AMPK is a major metabolic sensor that regulates glucose and lipid metabolism in response to nutrient and energy changes. It functions as a serine/threonine kinase and consists of a catalytic subunit (AMPK α) and two regulatory subunits (AMPK β and AMPK γ) [120]. AMPK is activated by metabolic stress and high intracellular levels of AMP, which leads to phosphorylation of the catalytic α-subunit (Threonine 172) by different upstream kinases [121]. As mention before, it has been shown that mTORC1 inhibits autophagy [117], while AMPK

induces autophagy [122]. It is well demonstrated, that AMPK suppresses mTORC1 activity by phosphorylation of TSC2 and Raptor, a subunit of mTORC1. This is thought to activate autophagy at low energy levels [123]. However, it has been recently reported that AMPK also activates autophagy through direct phosphorylation of ULK1, which is an important kinase in the autophagy formation process [124, 125]. Another study showed, that AMPK can induce autophagy at increased Ca^{2+} levels, even under normal energy levels [126]. Thus, the detailed molecular mechanisms in which AMPK activation induce autophagy in mammalian cells is not fully understood [121].

The tuberous sclerosis complex (TSC) is a heterodimer of TSC1 (also known as hamartin) and TSC2 protein (tuberin) and acts as a GTPase-activating protein (GAP) for the Rheb G-protein. [129]. In response to growth factor stimulation, the protein kinase AKT-1 becomes activated and inhibit TSC2 activity through phosphorylation. Thus, Rheb can then activate mTOR, leading to cell growth and division. However, in response to glucose deprivation and increased AMP levels, active AMPK phosphorylates and activates the TSC2 protein, which subsequently turns off the Rheb activity and mTORC1 signaling [130]. Previously, it has been shown, that *TSC2* gene expression can be induced by p53 in irradiation-treated HCT116 cells and temperature-sensitive V138/H1299 cells [116]. Hence, the regulation of TSC2 was further investigated in p53 +/+ and p53 -/- HepG2 cells. As shown in **Fig 11 B**, TSC2 mRNA levels slightly increased after 48h cultivation in both cell lines. However, the fold-change was less in p53 +/+ cells compared to p53 -/- cells. Surprisingly, 48h starvation notable reduced TSC2 mRNA levels in both cell lines. However, none of these differences were significant. Thus, these findings suggested that TSC2 expression is not regulated by p53 in HepG2 cells.

P53 has been reported to directly transactivate the damage-regulated autophagy modulator (DRAM). DRAM is a membrane protein and can localize to different organelles including the endoplasmic reticulum (ER) and lysosome [131]. Crighton et al demonstrated that DRAM is necessary for the ability of p53 to induce autophagy and to induce apoptosis in response to genotoxic stress [132]. Furthermore, Zhang et al. showed that mitochondria inhibitor 3-nitropropionic acid (3-NP) induced DRAM-mediated autophagy, which was largely dependent on p53. Fluorescence colocalization studies revealed that DRAM was predominantly localized at lysosomes, indicating that DRAM1 regulates autophagosome degradation through promoting lysosomal acidification and activation of lysosomal enzymes [133]. However, the exact mechanism by which DRAM1 mediates autophagy is not understood. Gene analysis of DRAM in HepG2 cells revealed an increase in p53 +/+ cells in response to starvation, while DRAM mRNA levels decrease in p53 -/- cells (**Fig 11 C**). This effect was also observed after 48h in normal culture medium, but the induction was less compared to the 48h starvation conditions. These results point to the probability that p53 is involved in DRAM gene expression under starvation.

Taken together, qPRC analysis of HepG2 cells revealed a moderate increase of *DRAM* in p53 +/+ cells after 48h of starvation which were blunted in p53 -/- cells, suggesting a link between p53 and the regulation of this gene in response to nutrient deprivation. However, the differences between p53 +/+ and p53 -/- cells were not statistically significant. Therefore, the role of p53 as transcriptional regulator of autophagy-related genes need to be studied further. Moreover, p53-regulated gene transcription is cell type- and stress-specific. For instance, Feng et al. showed that *TSC2* gene expression was highly induced in HCT116 cells after irradiation, while only marginal induction was seen in HepG2 cells. They further demonstrated that induction of AMPK β1, AMPK β2, *TSC2* and *PTEN* expression by p53 activation varies between different stress stimuli [116]. The identification of *DRAM* as p53 target gene has provided an important link between the regulation of autophagy and apoptotic cell death [134]. However, it was shown

that DRAM itself cannot induce apoptosis, indicating that p53 might activate *DRAM,* as well as other proapoptotic genes to promote a full cell-death response. Thus, further studies are required to determine how DRAM-induced autophagy contribute to apoptosis [132]. The link between DRAM and apoptosis suggests an important role for DRAM in tumor suppression. Indeed, it has been shown that expression of *DRAM* is downregulated in various cancer cells, including oral tumor lines and squamous cancers [132, 134]. Conversely, Lui et al. demonstrated that DRAM mRNA and protein levels were increased in HepG2 cells in response to starvation. They further showed that p53 was essential to induce DRAM-mediated autophagy, but DRAM-mediated autophagy was not able to induce apoptosis in response to starvation in HepG2 cells. Overall, these findings further demonstrate the complexity of p53 signaling.

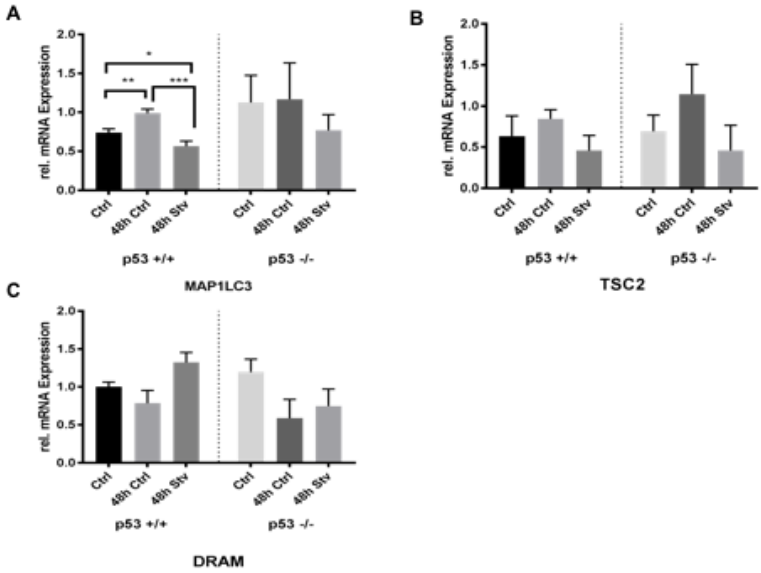

Figure 11: The regulation of MAP1LC3, TSC2 and DRAM expression by p53. qPCR analysis of *MAP1LC3*, *TSC*2 and *DRAM* in wildtype HepG2 (p53 +/+) and HepG2 clone 7 cells (p53 -/-) after 48h of starvation. Gene expression was normalized to GAPDH (n=3).

4.5.1 Potential cross-talk between p53 and mTOR signaling

Previously, it has been shown that mTORC1, a central regulator of nutrient and growth factor signaling, and p53, as key regulator of cellular stress, cross-talk with each other to coordinate cell growth, proliferation and apoptosis [112]. As mentioned in the previous paragraph, mTORC1 negatively regulates autophagy. The activity of mTORC1 can be inhibited by nutrient deprivation and the lipophilic macrolide Rapamycin by several mechanisms [135]. The regulation of mTORC1 is complex and include the action of PI3K-dependent kinase 1, AKT, and AMPK. In addition, it has been reported that p53 can inhibit mTORC1 activity through AMPK, which in turn activates TSC2 or by directly transactivating TSC2. TSC2 then inactivates mTORC1 signaling, leading to induction of autophagy [130]. These previous results prompted us to investigate the possible cross-talk between p53 and mTORC1 signaling in response to starvation in HepG2 cells. Therefore, HepG2 p53 +/+ and p53 -/- cells were subjected to either starvation medium or normal growth medium for 48h and were treated with Bafilomycin A (10nM) and/or Rapamycin (100nM).

Activated mTORC1 phosphorylates and activates the factor ribosomal protein S6 kinase-1 (P70S6K1). To monitor mTORC1 activity, the level of P70S6K1 phosphorylation was analyzed by Western Blot [136]. As shown in **Fig. 12 A**, P70S6K1 was phosphorylated in the 0h and 48h

control samples, indicating mTORC1 activity. Rapamycin specifically inhibit mTORC1 kinase activity, which is associated with reduced phosphorylation of P70S6K1 [135]. Indeed, Rapamycin treatment reduced the phosphorylation of P70S6K1. As expected, also nutrient deprivation reduced phosphorylation of P70S6K1, suggesting that the phosphorylation of P70S6K1 was mTORC1-specific. Treatment with Bafilomycin A1, which inhibits the last step autophagy, did not seem to affect mTORC1 activity in the 0h control samples. Interestingly, Bafilomycin treatment reduced the activation of P70S6K1 in the 48h control sample. In agreement with our results, Xu et al. showed that Bafilomycin inhibited EGF-stimulated mTORC1 activity, indicated by reduced phosphorylation of P70S6K. Notably, Bafilomycin-treatment did not change Akt or AMPK activity in their study. On the contrary, treatment with Bafilomycin caused a decrease of the intracellular concentration of essential amino acids, suggesting that Bafilomycin inhibited lysosomal proteolysis, leading to the blockage of mTORC1 activity. Since Bafilomycin is a potential inhibitor of the vacuolar ATPase, they further demonstrated that the blockage was caused by inhibition of vacuolar acidification. Therefore, they suggested that Bafilomycin blocked the proteasome-dependent proteolysis, leading to reduced intracellular levels of essential amino acids, which in turn inhibited EGF-induced mTORC1 activation [137]. Moreover, simultaneous incubation with Bafilomycin and Rapamycin mimicked the P70S4K1 levels of the samples, which were treated with either Rapamycin or Bafilomycin alone. Taken together, this suggested that both, Rapamycin and Bafilomycin, inhibit mTORC1 activity in HepG2 cells.

To investigate a potential connection between mTORC1 and autophagy in HepG2 cells, LC3-II protein levels were analyzed by Western Blot. Starvation and Rapamycin are well-known autophagy-inducers, resulting in increased LC3-II levels [70]. As expected, nutrient deprivation in presence and absence of Bafilomycin increased LC3-II levels. Also, treatment with Bafilomycin and Rapamycin in starved HepG2 cells slightly increased LC3-II protein levels. However, neither Bafilomycin nor Rapamycin alone stimulated an increase in LC3-II, as well as, co-treatment with Bafilomycin and Rapamycin did not affect LC3-II levels in nonstarved p53 +/+ cells. Moreover, it seemed that the autophagic flux was blocked under these experimental conditions. Noteworthy, a different Bafilomycin agent was used in this experiment (BioViotica BVT-0252 instead of Cayman #11038), which could be less efficient in HepG2 cells. Moreover, many factors can affect autophagic activity. According to Mizushima et al, the amount of LC3-II can vary greatly even when the same cell line is cultured in the same medium [31]. Thus, these data need to be interpreted with caution. Although Rapamycin treatment is widely used to induce autophagy, it has been shown that Rapamycin only exert partial effects with respect to autophagy induction [70]. Moreover, Thoreen et al, reported that Rapamycin was insensitive to inhibit mTORC1-mediated autophagy regulation [138]. For this reason, it would be of further interest to test a second-generation MTOR inhibitor, like Torin 1, which have shown to be more potent in most cell lines [78].

In addition to P70S6K and LC3, p53 protein levels were analyzed in the presence of Rapamycin. P53 protein levels slightly increased after 48h in normal growth medium. Neither Bafilomycin nor Rapamycin affected p53 protein levels under normal growth conditions. As expected, p53 strongly accumulated after 48h starvation. As observed in previous experiments, Bafilomycin treatment under nutrient deprivation decreased p53 stabilization. However, treatment of Rapamycin and co-treatment of Rapamycin and Bafilomycin strongly reduced p53 stabilization. Hence, it could be possible that these regimens induced p53 degradation, as seen in studies of Tasdemir et al. [86]. It has been shown that the mTOR pathway is deregulated in various cancer cells including hepatocellular carcinoma [139] and Rapamycin is recently used as therapeutic agent in cancer therapy [140]. In contrast, Kwon et al. have shown that Rapamycin inhibited cell proliferation of Huh7 cells by up-regulation of p53 protein levels, but

not mRNA levels, leading to down-regulation of the ERK1/2 signal. However, Rapamycin did not inhibit the proliferation of HepG2 cells [139]. These controversial findings indicate a need for further studies.

To further clarify the link between mTORC1 and p53 signaling, similar experiment to those carried out in p53 +/+ HepG2 cells were performed with p53 -/- HepG2 cells. As shown in **Fig 12 B**, treatment with Rapamycin and starvation conditions also decreased pP70S6K in p53 -/- cells, indicating inactivation of mTORC1. Surprisingly, treatment with Bafilomycin A resulted in phosphorylation of P70S6K1 in the 48h control cells. Since Bafilomycin treatment reduced mTORC1 activity in the p53 +/+ cells, but not in the p53 -/- cells, it could be possible, that p53 is required for this effect. As mentioned before, it has been shown that Bafilomycin may have off-target effects on mTORC1 regulation [78]. Previous studies suggested, that Bafilomycin at low concentration (5 nM) reduced phosphorylation of P70S6k in HepG2 cells by inhibition of the class I PI3K/Akt/mTOR/P70S6K signaling pathway [141]. Given that p53 and this signaling network communicate with each other [112], the downregulation mTORC1 by Bafilomycin may depend on p53. Furthermore, it is generally accepted that activated mTORC1 translocate to the lysosomal membrane where it forms a complex with vATPase [142]. Another recent study revealed that pharmacological inhibition of lysosomal activity by v-ATPase inhibitor Bafilomycin activated mTORC1 signaling in epiphyseal chondrocytes and they further showed that mTORC1 inhibition by lysosome v-ATPase activity was autophagy-independent [142]. However, there has been no clear evidence if mTORC1 inhibition of Bafilomycin is linked to p53. Hence, this needs to be formally proven.

Treatment of either Rapamycin and Bafilomycin, as well as co-treatment of Bafilomycin and Rapamycin did not change LC3-II protein levels in normal growth conditions in p53 -/- cells. Since Rapamycin was not sufficient to induce autophagy in wild-type HepG2 cells, it could be possible that the unchanged LC3-II protein levels upon Rapamycin treatment was due to the loss of p53 and not due to Rapamycin treatment. As seen in previous experiments, Bafilomycin treatment did not further increase LC3-II protein levels, suggesting stalled autophagy degradation under starvation.

Taken together, these results demonstrated that Rapamycin was not sufficient to induce autophagy in HepG2 cells. Thus, it was not possible to investigate whether the observed differences between p53 +/+ and p53 -/- cells were caused by deregulated mTORC1 signaling. Noteworthy, these data represented only a single experiment. Hence, this experiment need to be repeated, at least in triplicates, to test the link between p53 and mTOR signaling [143].

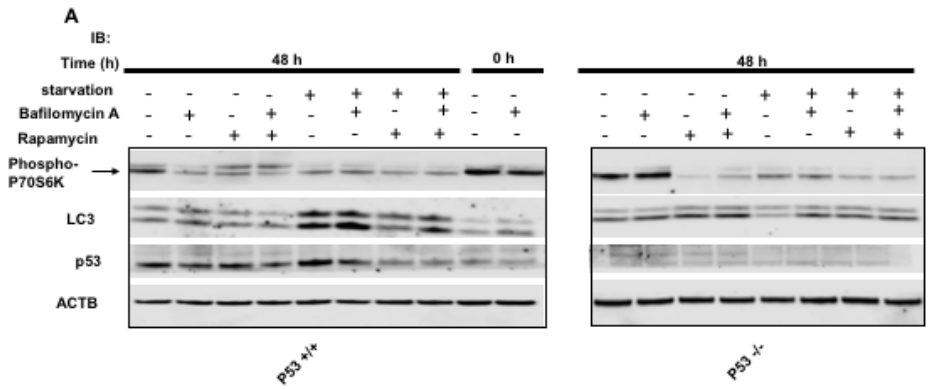

Figure 12: the cross-talk of p53 and mTOR signaling. P53 +/+ and p53 -/- cells were subjected to starvation medium for 48h and treated with 10 nM Bafilomycin A1 or 100 nM Rapamycin. Treatment were added 2h prior harvest. Protein samples were collected at indicated time points. Western blot analysis of pP70S6K, LC3, p53 and ACTB in p53 +/+ **(A)** and p53 -/- HepG2 cells **(B).** ACTB served as loading control. (n=1)

4.6 Monitoring autophagy in vivo by electron microscopy

To investigate the effect of p53 signaling on autophagy in physiological conditions, liver tissue of acute hepatic p53 loss-of-function mice models [42] were observed by electron microscopy. To induce autophagic activity, mice were starved for 24 hours, while a control group was fed *ad libitum*. As shown in **Fig 13 A and B,** fed mice had increased levels of liver glycogen, displayed as cauliflower-like structures [145]. However, it seemed that hepatic glycogen content was reduced in p53-deleted livers. Disturbances in glycogen storage has been observed previously in the same model [42], supporting the idea that hepatic p53 is involved in glucose homeostasis. Hepatic glycogen was not observed in both control and knockout mice after 24h of food withdrawal **(Fig 13 C and D**). Although lipid droplets could be observed in fed and fasted mice, the size of the lipid droplet was massively increased in the starved mice (**Fig 13 C and D**). Lipid droplets are the intracellular storage of neutral lipids and important for lipid metabolism and energy homeostasis. In starvation conditions, fatty acids, present as triglycerides in lipid droplets, fuel ATP production [146, 147]. In agreement with our results, Rambold et al. reported that the number and average lipid droplet size increased after 24h starvation in MEF cells and triglyceride storage was boosted [146] Strikingly, in addition to the massive lipid droplets, we observed small lipid droplets, which were surrounded by plasma membrane **(Fig 13 E and F).** Thus, it is tempting to speculate, that macroautophagy is involved in the degradation of these small lipid droplets. In agreement with this idea, Czaja et al revealed an association between lipid droplet components and autophagic compartments in livers of mice starved for increasing periods of time. They found that conjugation of LC3 occurred on the lipid droplet surface, leading to sequestration of only a portion of the lipid droplet. Moreover, they observed that lipid droplets were engulfed along with other cytosolic components [148]. The degradation of lipid droplets by autophagy is called lipophagy [147]. However, further studies are needed to clarify the role of autophagy in lipid droplet breakdown *in vivo* upon starvation. The lipid droplet containing vesicles could be observed in the control and p53-deleted livers. Hence, the exact role of p53 in hepatic lipid metabolism and lipophagy warrant further studies. By definition, autophagosomes are characterized as double-membrane-bound vesicles, containing cytoplasmic components [150]. In morphological studies, autophagosomes, amphisomes and autolysosomes are collectively termed autophagic vacuoles. These vesicles can be further classified into early autophagic vacuoles (AVi), containing morphologically intact cytosolic material, and late autophagic vacuoles (AVd), which display an altered ultrastructural appearance of the sequestered cytosolic content and increased electron density [30]. Accumulating evidence showed that starvation induced the greatest protein loss in the liver and that mice could lose 25%-40% of their liver protein in the first 48 h of starvation [34]. Surprisingly, only few autophagic structures could be observed after 24h of starvation in both, the control and the p53-depleted livers. Since autophagy is essential for the maintenance of cellular homeostasis [32], some autophagic vacuoles could also be observed in the fed cohorts. One explanation for the low autophagic activity could be that 24 hours of starvation is too long to monitor autophagy *in vivo* (Eskelinen, personal communication). Indeed, it is thought that macroautophagy is activated first in response to nutrient deprivation and upon prolonged starvation, the chaperone-mediated autophagy (CMA) takes over, while the activity of macroautophagy decreases [27]. CMA differs from macroautophagy in their selectivity towards cytosolic proteins harboring a KFERQ motif and the mechanism of delivery of the cargo to lysosomes [151]. The KFERQ- like motif of proteins is recognized and bind by the cytosolic chaperone heat shock cognate protein 70 (HSC70). After targeting, HSC70 mediates the

binding of the substrate protein to the cytosolic tail of the lysosomal membrane protein LAMP-2A. Subsequently, LAMP-2a assembles itself into a high molecular weight complex, which is thought to act as a translocation pore [27]. The substrate protein unfolds and crosses the lysosomal membrane into the lumen, where it is degraded [151]. In agreement with this idea, it has been shown that protein degradation by macroautophagy in the liver was rapidly activated during the first 4-6 h and declined after 8h of starvation. Then, hepatic CMA was gradually activated and reaches his maximum after 24h of starvation and remained activated for up to 3 days to deliver essential macromolecules [149]. Moreover, it has been shown that macroautophagy was still active in the liver after 8h of nutrient starvation, but the type of cargo sequestered by autophagosomes switched from proteins to lipids [152]. Hence, further studies focusing on CMA upon prolonged starvation in liver are needed to clarify when macroautophagy declines and CMA takes over. Noteworthy, the observation of autophagic vacuoles by electron microscopy only reflects the turnover status of the autophagosome at a given time. It has been reported that the half-life of an autophagosomes in liver is about 6-9 min [34]. Hence, it could be possible that we missed the timeframe, in which autophagic vacuoles exists. However, other studies could detect an increase in autophagy in the liver of mice starved for 24h [154]. Since the control and the p53-depleted liver displayed less autophagic structures than expected, it could be possible that the adenovirus, which was used to express either GFP as control or CRE in livers of adult mice, could negatively affect autophagy. However, there was no clear evidence that adenoviral-mediated knockdown influence autophagy in livers. Thus, further studies are needed to clarify the influence of the adenovirus-mediated expression of GFP and CRE in adult mice. A previous study showed that autophagic markers fluctuated excessively among individual mice after 24h of starvation. To prevent this fluctuation, autophagy induction was synchronized in all mice by using a starvation/feeding/re-starvation regimen, in which mice were starved for 24 h, fed for 2 h in the dark and then fasted again [155]. Hence, this experimental manipulation might enable the statistical analysis of experimental data in our settings.

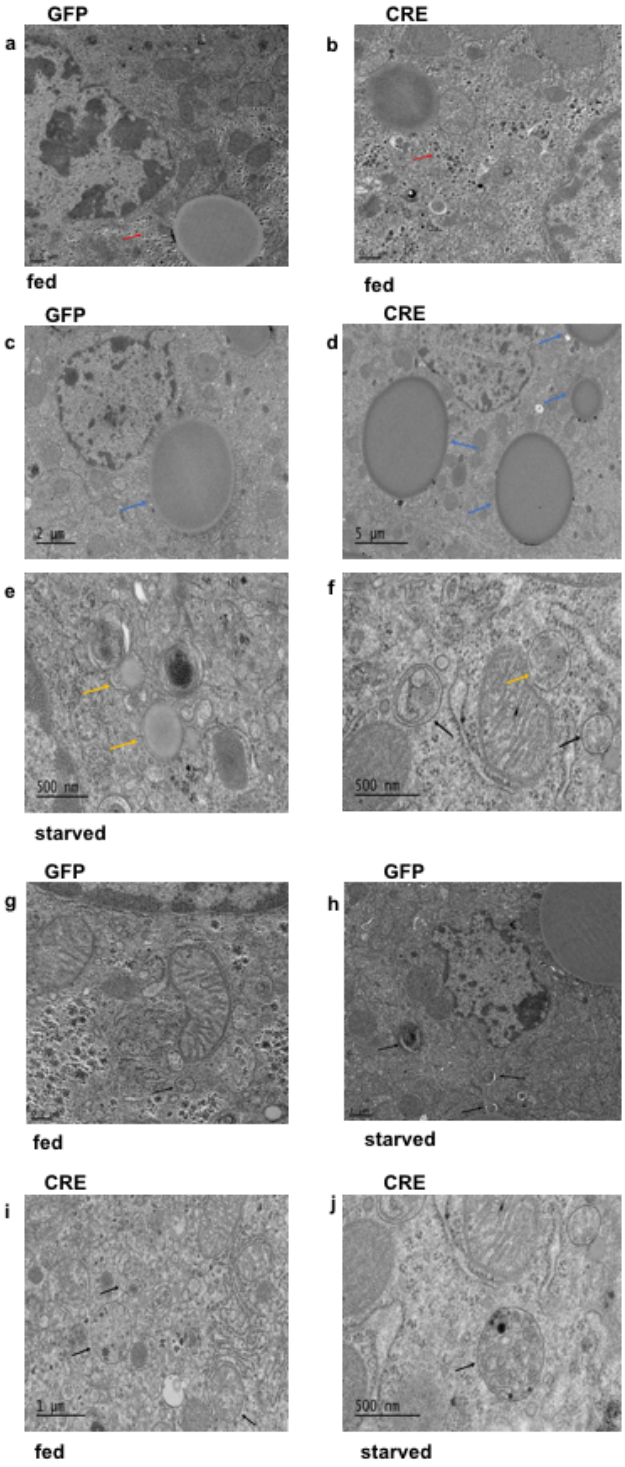

Figure 13: Monitoring autophagy in vivo by electron microscopy. P53 fl/fl mice were injected with adenoviral constructs expressing either GFP (control) or CRE (p53 deletion). Mice were fed *ad libitum* or starved for 24h. Liver were isolated and further processed for electron microscopy. **(A, B)** Glycogen content was visible in fed GFP and CRE livers, while no glycogen could be observed in starved livers (**C, D** red arrows) Lipid droplets were massively increased in starved liver samples (blue arrows in **D and C**) Small lipid droplets were surrounded by double-membrane vesicle in starved mice (yellow arrows in **E and F).** Autophagic vesicles could be detected in control and p53-depleted livers after 24h of starvation and upon feeding conditions (black arrows in **G, H, I, J)**

5 Conclusion and Open Questions

Accumulating evidence highlighted the complexity of p53 in metabolism regulation. In addition to its function as tumor suppressor [1, 2, 3], several novel p53 metabolic targets have been identified, implicating the importance of p53 in the regulation of cellular metabolism [144]. Recently, Prokesch et al. proposed that hepatic p53 protein is stabilized upon nutrient deprivation *in vivo* and *in vitro*. They further demonstrated that p53 was necessary for up-regulation of genes involved in amino acid catabolism and for maintenance of glucose homeostasis upon food withdrawal in mice, indicating a novel role of p53 regarding the physiological adaption to starvation [42]. It was therefore of interest, whether starvation-induced stabilization of p53 affects autophagy as possible downstream mechanism. Here, we showed that prolonged starvation significantly induces p53 stabilization in HepG2 cells. However, starvation and simultaneous treatment with Bafilomycin A, a well-known inhibitor of autophagy [69], revealed a significant decrease in p53 protein levels in HepG2. This effect was possibly due to the transfer of stress-stabilized p53 to mitochondria, leading to p53-dependent apoptosis [105]. Thus, to verify if p53 acts as an upstream regulator of autophagy, the effects of different autophagy inhibitors on p53 need to be investigated. LC3-II turnover assay revealed that depletion of p53 inhibit autophagic flux, suggesting the importance of p53 in autophagy. However, this assay is very sensitive and not all LC3-II is bound to autophagic membranes. Thus, further experiments, for example GFP-LC3 cleavage assays, need to be done to verify the observed results [70]. Previous studies indicate that p53 can either induce or inhibit autophagy, depending on its subcellular localization [40, 86, 89]. Cytoplasmic p53 seems to suppress autophagy, while nuclear p53 is associated with autophagy induction [2]. Hence, it is tempting to speculate that nuclear p53 is associated with the observed autophagy induction in HepG2 cells upon starvation. Tasdemir et al demonstrated, that cytosolic p53 was degraded in presence of various autophagy inducers [89]. Here we observed that autophagy inducers, such as starvation or Rapamycin, did not cause p53 degradation, suggesting that nuclear, not cytoplasmic p53 might be associated with autophagy regulation in HepG2 cells. However, both, autophagy and p53 stabilization can be induced by different stress stimuli and it could be possible that these two pathways are stimulated independently of each other. Hence, these data warrant further studies to clarify the exact role of p53 in autophagy regulation. Strikingly, p53 seems to promote the downregulation of LC3 mRNA under conditions of prolonged starvation in HepG2 cells. Although the observed decrease of LC3 gene expression is contrary to the observed increase of LC3 protein upon starvation, this could be irrelevant since most ATG genes are post-translational regulated rather than transcriptional [113]. Hence, the impact of p53 on post-transcriptional processes should be further investigated. In addition, gene expression of TSC2 and DRAM was not regulated significantly by p53 in HepG2 cells. However, transcriptional regulation of p53 is cell type- and stress specific [116]. Thus, gene expression analysis of other p53 target genes, including PTEN, AMPKβ, or p21 would be of great interest.

Previous studies have shown that induction of autophagy by p53 is linked to mTORC1 signaling [89]. However, mTORC1 signaling, autophagy, and p53 signaling are very complex and context-specific pathways, and we cannot answer the question how these pathways communicate with each other in HepG2 cells. Moreover, HepG2 cells are characterized as hepatoma cell line [53]. mTORC1, autophagy and p53 signaling are important regulators of cellular homeostasis and cancer development is often associated with deregulation of any of those pathways [146]. Therefore, all observed results need to be interpreted with caution.
Altogether, our findings imply that p53 stabilization is linked to autophagy induction upon prolonged starvation in HepG2 cells. Furthermore, the data represented here provide a basis for further experiments on revealing the underlying mechanism of p53 and autophagy.

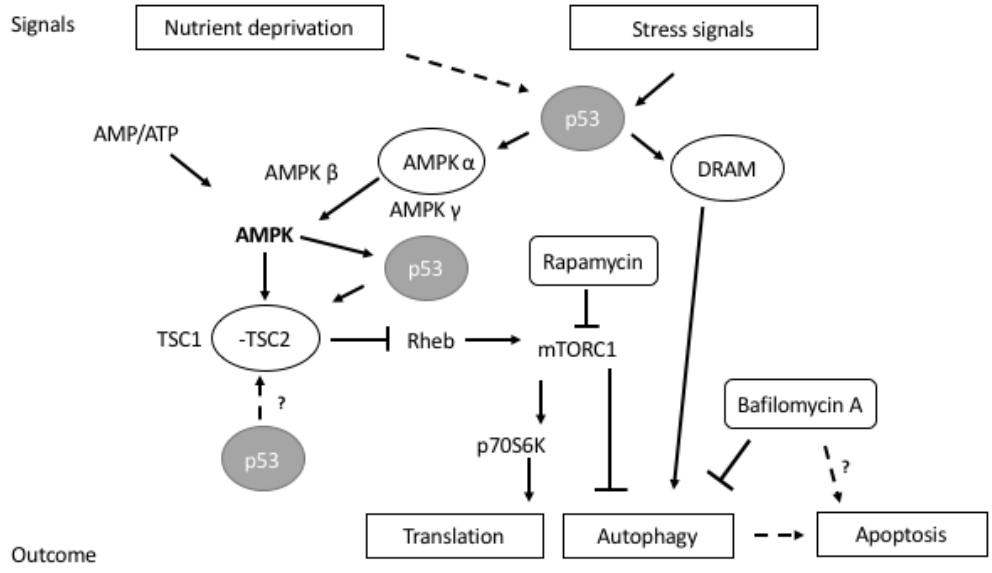

Figure 14: the coordinate communication between p53 signaling and autophagy regulation. A diagram of the cross-talks between the p53 pathway and other signaling pathways including mTOR and AMPK signaling.

6 References

1. Brady, C. A., & Attardi, L. D. (2010). p53 at a glance. *Journal of Cell Science*, *123 VN*-(15), 2527–2532. https://doi.org/10.1242/jcs.064501
2. Berkers, C. R., Maddocks, O. D. K., Cheung, E. C., Mor, I., & Vousden, K. H. (2013). Metabolic regulation by p53 family members. *Cell Metabolism*, *18*(5), 617–633. https://doi.org/10.1016/j.cmet.2013.06.019
3. Brooks, C. L., & Gu, W. (2010). New insights into p53 activation. *Cell Research*, *20*(6), 614–621. http://dx.doi.org/10.1038/cr.2010.53
4. Mihara, M., Erster, S., Zaika, A., Petrenko, O., Chittenden, T., Pancoska, P., & Moll, U. M. (2017). p53 Has a Direct Apoptogenic Role at the Mitochondria. *Molecular Cell*, *11*(3), 577–590. https://doi.org/10.1016/S1097-2765(03)00050-9
5. Chipuk, J. E., Bouchier-Hayes, L., Kuwana, T., Newmeyer, D. D., & Green, D. R. (2005). PUMA Couples the Nuclear and Cytoplasmic Proapoptotic Function of p53. *Science*, *309*(5741), 1732 LP-1735. http://science.sciencemag.org/content/309/5741/1732.
6. Janz, C., & Wiesmüller, L. (2002). Wild-type p53 inhibits replication-associated homologous recombination. *Oncogene*, *21*(38), 5929–33. https://doi.org/10.1038/sj.onc.1205757
7. Suzuki, H. I., Yamagata, K., Sugimoto, K., Iwamoto, T., Kato, S., & Miyazono, K. (2009). Modulation of microRNA processing by p53. *Nature*, *460*(7254), 529–533. http://dx.doi.org/10.1038/nature08199
8. Wen Xue. 7.344 Tumor Suppressor Gene p53: How the Guardian of our Genome Prevents Cancer. Fall 2010. Massachusetts Institute of Technology: MIT OpenCourseWare, https://ocw.mit.edu. License: Creative Commons BY-NC-SA.
9. Bensaad, K., Tsuruta, A., Selak, M. A., Vidal, M. N. C., Nakano, K., Bartrons, R., … Vousden, K. H. (2006). TIGAR, a p53-inducible regulator of glycolysis and apoptosis. *Cell*, *126*(1), 107–120. https://doi.org/10.1016/j.cell.2006.05.036
10. Matoba, S., Kang, J.-G., Patino, W. D., Wragg, A., Boehm, M., Gavrilova, O., … Hwang, P. M. (2006). p53 Regulates Mitochondrial Respiration. *Science*, *312*(5780), 1650 LP-1653. http://science.sciencemag.org/content/312/5780/1650.
11. Jiang, P., Du, W., Wang, X., Mancuso, A., Gao, X., Wu, M., & Yang, X. (2011). p53 regulates biosynthesis through direct inactivation of glucose-6-phosphate dehydrogenase. *Nat Cell Biol*, *13*(3), 310–316. http://dx.doi.org/10.1038/ncb2172
12. Parrales, A., & Iwakuma, T. (2016). p53 as a Regulator of Lipid Metabolism in Cancer. (G. Drummen, Ed.), *International Journal of Molecular* http://doi.org/10.3390/ijms17122074
13. Liu, J., Zhang, C., Hu, W., & Feng, Z. (2015). Tumor suppressor p53 and its mutants in cancer metabolism. *Cancer Letters*. https://doi.org/10.1016/j.canlet.2013.12.025
14. Goldstein, I., & Rotter, V. (n.d.). Regulation of lipid metabolism by p53 - fighting two villains with one sword. *Trends in Endocrinology and Metabolism*, *23*(11), 567–575. https://doi.org/10.1016/j.tem.2012.06.007
15. Vousden, K. H., & Ryan, K. M. (2009). P53 and Metabolism. *Nature Reviews. Cancer*, *9*(10), 691–700. https://doi.org/10.1038/nrc2715
16. Yahagi, N., Shimano, H., Matsuzaka, T., Sekiya, M., Najima, Y., Okazaki, S., … Yamada, N. (2004). p53 Involvement in the Pathogenesis of Fatty Liver Disease. *Journal of Biological Chemistry*, *279*(20), 20571–20575. https://doi.org/10.1074/jbc.M400884200
17. Guevara, N. V, Kim, H.-S., Antonova, E. I., & Chan, L. (1999). The absence of p53 accelerates atherosclerosis by increasing cell proliferation in vivo. *Nat Med*, *5*(3), 335–339. http://dx.doi.org/10.1038/6585

18. Schupp, M., Chen, F., Briggs, E. R., Rao, S., Pelzmann, H. J., Pessentheiner, A. R., … Prokesch, A. (2013). Metabolite and transcriptome analysis during fasting suggest a role for the p53-Ddit4 axis in major metabolic tissues. *BMC Genomics*, *14*, 758. https://doi.org/10.1186/1471-2164-14-758
19. Zaffagnini, G., & Martens, S. (2016). Mechanisms of Selective Autophagy. Journal of Molecular Biology, 428(9Part A), 1714–1724. http://doi.org/10.1016/j.jmb.2016.02.004
20. Russell, R. C., Yuan, H.-X., & Guan, K.-L. (2014). Autophagy regulation by nutrient signaling. *Cell Research*, *24*(1), 42–57. https://doi.org/10.1038/cr.2013.166
21. Hamasaki, M., Furuta, N., Matsuda, A., Nezu, A., Yamamoto, A., Fujita, N., … Yoshimori, T. (2013). Autophagosomes form at ER-mitochondria contact sites. *Nature*, *495*(7441), 389–393. http://dx.doi.org/10.1038/nature11910
22. Ravikumar, B., Moreau, K., Jahreiss, L., Puri, C., & Rubinsztein, D. C. (2010). Plasma membrane contributes to the formation of pre-autophagosomal structures. *Nat Cell Biol*, *12*(8), 747–757. http://dx.doi.org/10.1038/ncb2078
23. Yla-Anttila, P., Vihinen, H., Jokitalo, E., & Eskelinen, E.-L. (2009). 3D tomography reveals connections between the phagophore and endoplasmic reticulum. *Autophagy*, *5*(8), 1180–1185.
24. Karanasios, E., Stapleton, E., Manifava, M., Kaizuka, T., Mizushima, N., Walker, S. A., & Ktistakis, N. T. (2013). Dynamic association of the ULK1 complex with omegasomes during autophagy induction. *Journal of Cell Science*, *126*(22), 5224 LP-5238. http://jcs.biologists.org/content/126/22/5224
25. Mehrpour, M., Esclatine, A., Beau, I., & Codogno, P. (2010). Overview of macroautophagy regulation in mammalian cells. *Cell Res*, *20*(7), 748–762. http://dx.doi.org/10.1038/cr.2010.82
26. Martens, S., Nakamura, S., & Yoshimori, T. (2016). Phospholipids in Autophagosome Formation and Fusion. *Journal of Molecular Biology*, *428*(24, Part A), 4819–4827. http://dx.doi.org/10.1016/j.jmb.2016.10.029
27. Damme, M., Suntio, T., Saftig, P., & Eskelinen, E. L. (2014). Autophagy in neuronal cells: general principles and physiological and pathological functions. *Acta Neuropathologica*, *129*(3), 337–362. https://doi.org/10.1007/s00401-014-1361-4
28. Tanida, I., Ueno, T., & Kominami, E. (2008). LC3 and Autophagy. In V. Deretic (Ed.), *Autophagosome and Phagosome* (pp. 77–88). Totowa, NJ: Humana Press. https://doi.org/10.1007/978-1-59745-157-4_4
29. Müller, M., Schmidt, O., Angelova, M., Faserl, K., Weys, S., Kremser, L., … Teis, D. (2015). The coordinated action of the MVB pathway and autophagy ensures cell survival during starvation. *eLife*, *4*, e07736. https://doi.org/10.7554/eLife.07736
30. Eskelinen, E. L. (2005). Maturation of autophagic vacuoles in Mammalian cells. *Autophagy*, *1*(1), 1–10. https://doi.org/10.4161/auto.1.1.1270
31. Mizushima, N., & Yoshimori, T. (2007). How to Interpret LC3 Immunoblotting ND RIB ND ES SC RIB. *Autophagy*, *3*(December), 4–7. https://doi.org/10.4161/auto.4600
32. Todde, V., Veenhuis, M., & van der Klei, I. J. (2009). Autophagy: Principles and significance in health and disease. *Biochimica et Biophysica Acta (BBA) - Molecular Basis of Disease*, *1792*(1), 3–13. http://dx.doi.org/10.1016/j.bbadis.2008.10.016
33. Rabinowitz, J. D., & White, E. (2010). Autophagy and Metabolism. *Science (New York, N.Y.)*, *330*(6009), 1344–1348. https://doi.org/10.1126/science.1193497
34. Yin, X. M., Ding, W. X., & Gao, W. (2008). Autophagy in the liver. *Hepatology*, *47*(5), 1773–1785. https://doi.org/10.1002/hep.22146
35. The Nobel Assembly at Karolinska Institute. (2016). Discoveries of Mechanisms for Autophagy, 1–5.
36. Komatsu, M. (2012). Liver autophagy: physiology and pathology. *The Journal of Biochemistry*, *152*(1), 5–15. http://dx.doi.org/10.1093/jb/mvs059

37. Codogno, P., & Meijer, A. J. (2013). Autophagy in the liver. *Journal of Hepatology*, *59*(2), 389–391. http://dx.doi.org/10.1016/j.jhep.2013.02.031
38. Czaja, M. J. (2011). Functions of autophagy in hepatic and pancreatic physiology and disease. *Gastroenterology*, *140*(7), 1895–1908. https://doi.org/10.1053/j.gastro.2011.04.038
39. Maiuri, M. C., Tasdemir, E., Criollo, A., Morselli, E., Vicencio, J. M., Carnuccio, R., & Kroemer, G. (2008). Control of autophagy by oncogenes and tumor suppressor genes. *Cell Death Differ*, *16*(1), 87–93. http://dx.doi.org/10.1038/cdd.2008.131
40. Maiuri, M. C., Galluzzi, L., Morselli, E., Kepp, O., Malik, S. A., & Kroemer, G. (2010). Autophagy regulation by p53. *Current Opinion in Cell Biology*, *22*(2), 181–185. https://doi.org/10.1016/j.ceb.2009.12.001
41. Scherz-Shouval, R., Weidberg, H., Gonen, C., Wilder, S., Elazar, Z., & Oren, M. (2010). p53-dependent regulation of autophagy protein LC3 supports cancer cell survival under prolonged starvation. *Proceedings of the National Academy of Sciences of the United States of America*, *107*(43), 18511–18516. https://doi.org/10.1073/pnas.1006124107
42. Prokesch, A., Graef, F. A., Madl, T., Kahlhofer, J., Heidenreich, S., Schumann, A., … Schupp, M. (2016). Liver p53 is stabilized upon starvation and required for amino acid catabolism and gluconeogenesis. *The FASEB Journal*. https://doi.org/10.1096/fj.201600845R
43. Wu, J. C., Merlino, G., & Fausto, N. (1994). Establishment and characterization of differentiated, nontransformed hepatocyte cell lines derived from mice transgenic for transforming growth factor alpha. *Proceedings of the National Academy of Sciences of the United States of America*, *91*(2), 674–678. https://doi.org/10.1073/pnas.91.2.674
44. Dumenco, L., Oguey, D., Wu, J., Messier, N., & Fausto, N. (1995). Introduction of a murine p53 mutation corresponding to human codon 249 into a murine hepatocyte cell line results in growth advantage, but not in transformation. *Hepatology*, *22*(4 PART 1), 1279–1288. https://doi.org/10.1016/0270-9139(95)90640-1
45. Goldstein, I., & Hager, G. L. (2016). Transcriptional and Chromatin Regulation during Fasting - The Genomic Era. *Trends in Endocrinology & Metabolism*, *26*(12), 699–710. https://doi.org/10.1016/j.tem.2015.09.005
46. Su, X., Gi, Y. J., Chakravarti, D., Chan, I. L., Zhang, A., Xia, X., … Flores, E. R. (2012). TAp63 is a master transcriptional regulator of lipid and glucose metabolism. *Cell Metabolism*, *16*(4), 511–525. https://doi.org/10.1016/j.cmet.2012.09.006
47. Kanfi, Y., Peshti, V., Gozlan, Y. M., Rathaus, M., Gil, R., & Cohen, H. Y. (2008). Regulation of SIRT1 protein levels by nutrient availability. *FEBS Letters*, *582*(16), 2417–2423. https://doi.org/10.1016/j.febslet.2008.06.005
48. Kottakis, F., & Bardeesy, N. (2012). LKB1-AMPK axis revisited. *Cell Research*, *22*(12), 1617–1620. https://doi.org/10.1038/cr.2012.108
49. Lu, T.-L., Huang, G.-J., Wang, H.-J., Chen, J.-L., Hsu, H.-P., & Lu, T.-J. (2010). Hispolon promotes MDM2 downregulation through chaperone-mediated autophagy. *Biochemical and Biophysical Research Communications*, *398*(1), 26–31. http://dx.doi.org/10.1016/j.bbrc.2010.06.004
50. Alexander, A., & Walker, C. L. (2011). The role of LKB1 and AMPK in cellular responses to stress and damage. *FEBS Letters*, *585*(7), 952–957. http://dx.doi.org/10.1016/j.febslet.2011.03.010
51. Gonfloni, S., Caputo, V., & Iannizzotto, V. (2015). P63 in health and cancer. *International Journal of Developmental Biology*, *59*(1–3), 87–93. https://doi.org/10.1387/ijdb.150045sg
52. Gaiddon, C., Lokshin, M., Ahn, J., Zhang, T., & Prives, C. (2001). A subset of tumor-derived mutant forms of p53 down-regulate p63 and p73 through a direct interaction with

the p53 core domain. *Molecular and Cellular Biology*, *21*(5), 1874–1887. https://doi.org/10.1128/MCB.21.5.1874-1887.2001
53. Maurel, P., (2010). Hepatocytes: Methods and Protocols (Preface 7-9). *Methods Mol Biol,* 640:7-9. doi:10.1007/978-1-60761-688-7_3
54. Klein, S., Mueller, D., Schevchenko, V., & Noor, F. (2014). Long-term maintenance of HepaRG cells in serum-free conditions and application in a repeated dose study. *Journal of Applied Toxicology*. https://doi.org/10.1002/jat.2929
55. Lereau, M., Gouas, D., Villar, S., Besaratinia, A., Hautefeuille, A., Berthillon, P., … Chemin, I. (2012). Interactions between hepatitis B virus and aflatoxin B 1: Effects on p53 induction in hepaRG cells. *Journal of General Virology*, *93*(3), 640–650. https://doi.org/10.1099/vir.0.032482-0
56. Marion, M.-J., Hantz, O., & Durantel, D. (2010). The HepaRG cell line: biological properties and relevance as a tool for cell biology, drug metabolism, and virology studies. *Methods Mol Biol,* 640:261–272. https://doi.org/10.1007/978-1-60761-688-7_13
57. Gripon, P., Rumin, S., Urban, S., Le Seyec, J., Glaise, D., Cannie, I., … Guguen-Guillouzo, C. (2002). Infection of a human hepatoma cell line by hepatitis B virus. *Proceedings of the National Academy of Sciences*, *99*(24), 15655–15660. https://doi.org/10.1073/pnas.232137699
58. Bednarkiewicz, A., Rodrigues, R. M., & Whelan, M. P. (2010). Enrichment of hepatocytes in a HepaRG culture using spatially selective photodynamic treatment. *Journal of Biomedical Optics*, *15*(2), 28002–28007. http://dx.doi.org/10.1117/1.3369000
59. Biopredic International, St. Gregorie, France. Frequently Asked Questions. http://www.heparg.com/index.php?rub=frequently_asked_questions
60. Parent, R., Marion, M.-J., Furio, L., Trépo, C., & Petit, M.-A. (2017). Origin and characterization of a human bipotent liver progenitor cell line. *Gastroenterology*, *126*(4), 1147–1156. https://doi.org/10.1053/j.gastro.2004.01.002
61. Cerec, V., Glaise, D., Garnier, D., Morosan, S., Turlin, B., Drenou, B., … Corlu, A. (2007). Transdifferentiation of hepatocyte-like cells from the human hepatoma hepaRG cell line through bipotent progenitor. *Hepatology*, *45*(4), 957–967. https://doi.org/10.1002/hep.21536
62. Gilot, D., Loyer, P., Corlu, A., Glaise, D., Lagadic-Gossmann, D., Atfi, A., … Guguen-Guillouzo, C. (2002). Liver protection from apoptosis requires both blockage of initiator caspase activities and inhibition of ASK1/JNK pathway via glutathione S-transferase regulation. *The Journal of Biological Chemistry*, *277*(51), 49220–49229. https://doi.org/10.1074/jbc.M207325200
63. Parent, R., Kolippakkam, D., Booth, G., & Beretta, L. (2007). Mammalian target of rapamycin activation impairs hepatocytic differentiation and targets genes moderating lipid homeostasis and hepatocellular growth. Cancer Research, 67(9), 4337–4345. https://doi.org/10.1158/0008-5472.CAN-06-3640
64. Feng, Z. (2010). p53 Regulation of the IGF-1/AKT/mTOR Pathways and the Endosomal Compartment. *Cold Spring Harbor Perspectives in Biology*, *2*(2), a001057. https://doi.org/10.1101/cshperspect.a001057
65. Levy, G., Bomze, D., Heinz, S., Ramachandran, S. D., Noerenberg, A., Cohen, M., … Nahmias, Y. (2015). Long-term culture and expansion of primary human hepatocytes. *Nature Biotechnology*, *33*(12), 1264–1271. https://doi.org/10.1038/nbt.3377
66. Tolosa, L., Gomez-Lechon, M. J., Lopez, S., Guzman, C., Castell, J. V., Donato, M. T., & Jover, R. (2016). Human Upcyte hepatocytes: Characterization of the hepatic phenotype and evaluation for acute and long-term hepatotoxicity routine testing. *Toxicological Sciences*, *152*(1), 214–229. https://doi.org/10.1093/toxsci/kfw078

67. Perry, M. E. (2010). The regulation of the p53-mediated stress response by MDM2 and MDM4. *Cold Spring Harbor Perspectives in Biology*, *2*(1), a000968. https://doi.org/10.1101/cshperspect.a000968
68. Barth, S., Glick, D., & Macleod, K. F. (2010). Autophagy: Assays and artifacts. *Journal of Pathology*, *221*(2), 117–124. https://doi.org/10.1002/path.2694
69. Mauvezin, C., & Neufeld, T. P. (2015). Bafilomycin A1 disrupts autophagic flux by inhibiting both V-ATPase-dependent acidification and Ca-P60A/SERCA-dependent autophagosome-lysosome fusion. *Autophagy*, *11*(8), 1437–1438. https://doi.org/10.1080/15548627.2015.1066957
70. Mizushima, N., Yoshimori, T., & Levine, B. (2017). Methods in Mammalian Autophagy Research. *Cell*, *140*(3), 313–326. https://doi.org/10.1016/j.cell.2010.01.028
71. Romero-Calvo, I., Ocón, B., Martínez-Moya, P., Suárez, M. D., Zarzuelo, A., Martínez-Augustin, O., & de Medina, F. S. (2010). Reversible Ponceau staining as a loading control alternative to actin in Western blots. *Analytical Biochemistry*, *401*(2), 318–320. http://dx.doi.org/10.1016/j.ab.2010.02.036
72. Hardie, D. G., Ross, F. A., & Hawley, S. A. (2012). AMPK: a nutrient and energy sensor that maintains energy homeostasis. *Nat Rev Mol Cell Biol*, *13*(4), 251–262. http://dx.doi.org/10.1038/nrm3311
73. Qiu, G.-H., Xie, X., Xu, F., Shi, X., Wang, Y., & Deng, L. (2015). Distinctive pharmacological differences between liver cancer cell lines HepG2 and Hep3B. *Cytotechnology*, *67*(1), 1–12. https://doi.org/10.1007/s10616-014-9761-9
74. Dugina, V., Zwaenepoel, I., Gabbiani, G., Clement, S., & Chaponnier, C. (2009). Beta and gamma-cytoplasmic actins display distinct distribution and functional diversity. *Journal of Cell Science*, *122*(Pt 16), 2980–2988. https://doi.org/10.1242/jcs.041970
75. Walker, J. M. (1994). The bicinchoninic acid (BCA) assay for protein quantitation. *Methods in Molecular Biology (Clifton, N.J.)*, *32*, 5–8. https://doi.org/10.1385/0-89603-268-X:5
76. Martinet, W. (2006). In Situ Detection of Starvation-induced Autophagy. *Journal of Histochemistry and Cytochemistry*, *54*(1), 85–96. https://doi.org/10.1369/jhc.5A6743.2005
77. Kristensen, A. R., Schandorff, S., Høyer-Hansen, M., Nielsen, M. O., Jäättelä, M., Dengjel, J., & Andersen, J. S. (2008). Ordered organelle degradation during starvation-induced autophagy. *Molecular & Cellular Proteomics : MCP*, *7*(12), 2419–2428. https://doi.org/10.1074/mcp.M800184-MCP200
78. Klionsky DJ, Abdelmohsen K, Abe A, Abedin MJ, Abeliovich H, Acevedo Arozena A, Adachi H, Adams CM, Adams PD, Adeli K, Adhihetty PJ, Adler SG, Agam G, Agarwal R, Aghi MK, Agnello M, Agostinis P, Aguilar PV, Aguirre-Ghiso J, Airoldi EM, Ait-Si-Ali S, Akemat, Z. S. (2016). Guidelines for use and interpretation of assays for monitoring autophagy (3rd edition). *Autophagy*, *12*(1), 1–222. https://doi.org/10.1080/15548627.2015.1100356
79. Sengupta, S., Peterson, T. R., & Sabatini, D. M. (2010). Regulation of the mTOR complex 1 pathway by nutrients, growth factors, and stress. *Molecular Cell*, *40*(2), 310–322. https://doi.org/10.1016/j.molcel.2010.09.026
80. Laplante, M., & Sabatini, D. M. (2009). mTOR signaling at a glance. *Journal of Cell Science*, *122*(20), 3589 LP-3594. http://jcs.biologists.org/content/122/20/3589
81. Eberhart, K., Oral, O., & Gozuacik, D. (2013). *Autophagy: Chapter 13. Induction of Autophagic Cell Death by Anticancer Agents*. Elsevier Science. Retrieved from https://books.google.fi/books?id=AIpzDAAAQBAJ
82. Kawauchi, K., Araki, K., Tobiume, K., & Tanaka, N. (2008). p53 regulates glucose metabolism through an IKK-NF-kappaB pathway and inhibits cell transformation. *Nature Cell Biology*, *10*(5), 611–618. https://doi.org/10.1038/ncb1724

83. Wang, D., Peng, Z., Ren, G., & Wang, G. (2015). The different roles of selective autophagic protein degradation in mammalian cells. *Oncotarget*, *6*(35), 37098–116. https://doi.org/10.18632/oncotarget.5776
84. Fimia, G., Kroemer, G., & Piacentini, M. (2013). Molecular mechanisms of selective autophagy. *Cell Death and Differentiation*, *20*(1), 1–2. https://doi.org/10.1038/cdd.2012.97
85. Park, C., & Cuervo, A. M. (2013). Selective Autophagy: Talking with the UPS. *Cell Biochemistry and Biophysics*, *67*(1), 3–13. https://doi.org/10.1007/s12013-013-9623-7
86. Tasdemir, E., Maiuri, M. C., Morselli, E., Criollo, A., D'Amelio, M., Djavaheri-Mergny, M., … Kroemer, G. (2008). A dual role of p53 in the control of autophagy. *Autophagy*, *4*(6), 810–814. https://doi.org/10.4161/auto.6486
87. Lazo, P. A. (2017). Reverting p53 activation after recovery of cellular stress to resume with cell cycle progression. *Cellular Signalling*, *33*, 49–58. https://doi.org/10.1016/j.cellsig.2017.02.005
88. Green, D. R., & Kroemer, G. (2009). Cytoplasmic functions of the tumor suppressor p53. *Nature*, *458*(7242), 1127. https://doi.org/10.1038/nature07986
89. Tasdemir, E., Maiuri, M. C., Galluzzi, L., Vitale, I., Djavaheri-mergny, M., Amelio, M. D., … Madeo, F. (2009). Regulation of autophagy by cytoplasmic p53. *Nature Cell Biology*, *10*(6), 676–687. https://doi.org/10.1038/ncb1730
90. Gao, W., Shen, Z., Shang, L., & Wang, X. (2011). Upregulation of human autophagy-initiation kinase ULK1 by tumor suppressor p53 contributes to DNA-damage-induced cell death. *Cell Death and Differentiation*, *18*(10), 1598–1607. https://doi.org/10.1038/cdd.2011.33
91. Streeter, A., Menzies, F. M., & Rubinsztein, D. C. (2016). LC3-II Tagging and Western Blotting for Monitoring Autophagic Activity in Mammalian Cells. *Methods in Molecular Biology (Clifton, N.J.)*, *1303*, 161–170. https://doi.org/10.1007/978-1-4939-2627-5_8
92. Mizushima, N., Overview: autophagy methods in mammals. http://proteolysis.jp/autophagy/protocol/protocol%20files/Overview%20for%20autophagy%20analysis%20in%20mammals.pdf
93. Yoshimori, T., Yamamoto, A., Moriyama, Y., Futai, M., & Tashiro, Y. (1991). Bafilomycin A1, a specific inhibitor of vacuolar-type H(+)-ATPase, inhibits acidification and protein degradation in lysosomes of cultured cells. *The Journal of Biological Chemistry*, *266*(26), 17707–17712.
94. Tanida, I., Ueno, T., & Kominami, E. (2008). LC3 and Autophagy. *Methods in Molecular Biology (Clifton, N.J.)*, *445*, 77–88. https://doi.org/10.1007/978-1-59745-157-4_4
95. Metz, P., Chiramel, A., Chatel-Chaix, L., Alvisi, G., Bankhead, P., Mora-Rodríguez, R., … Bartenschlager, R. (2015). Dengue virus inhibition of autophagic flux and dependency of viral replication on proteasomal degradation of the autophagy receptor p62. *Journal of Virology*, *89*(15), JVI.00787-15. https://doi.org/10.1128/JVI.00787-15
96. Sharifi, M. N., Mowers, E. E., Drake, L. E., & Macleod, K. F. (2015). Measuring Autophagy in Stressed Cells. *Methods in Molecular Biology (Clifton, N.J.)*, *1292*, 129–150. https://doi.org/10.1007/978-1-4939-2522-3_10
97. Chittaranjan, S., Bortnik, S., & Gorski, S. M. (2015). Monitoring Autophagic Flux by Using Lysosomal Inhibitors and Western Blotting of Endogenous MAP1LC3B. *Cold Spring Harbor Protocols*, *2015*(8), pdb.prot086256. https://doi.org/10.1101/pdb.prot086256
98. Abounit, K., Scarabelli, T. M., & McCauley, R. B. (2012). Autophagy in mammalian cells. *World Journal of Biological Chemistry*, *3*(1), 1–6. https://www.ncbi.nlm.nih.gov/pmc/articles/PMC3272585/

99. White, E. (2012). Deconvoluting the context-dependent role for autophagy in cancer. *Nature Reviews. Cancer*, *12*(6), 401–410. https://doi.org/10.1038/nrc3262
100. Yang, H., Peng, Y.-F., Ni, H.-M., Li, Y., Shi, Y.-H., Ding, W.-X., & Fan, J. (2015). Basal Autophagy and Feedback Activation of Akt Are Associated with Resistance to Metformin-Induced Inhibition of Hepatic Tumor Cell Growth. *PLoS ONE*, *10*(6), e0130953. https://doi.org/10.1371/journal.pone.0130953
101. Loos, B., du Toit, A., & Hofmeyr, J.-H. S. (2014). Defining and measuring autophagosome flux—concept and reality. *Autophagy*, *10*(11), 2087–96. https://doi.org/10.4161/15548627.2014.973338
102. Boya, P., Gonzalez-Polo, R.-A., Poncet, D., Andreau, K., Vieira, H. L. A., Roumier, T., … Kroemer, G. (2003). Mitochondrial membrane permeabilization is a critical step of lysosome-initiated apoptosis induced by hydroxychloroquine. *Oncogene*, *22*(25), 3927–3936. https://doi.org/10.1038/sj.onc.1206622
103. Boya, P., Gonzalez-Polo, R.-A., Casares, N., Perfettini, J.-L., Dessen, P., Larochette, N., … Kroemer, G. (2005). Inhibition of macroautophagy triggers apoptosis. *Molecular and Cellular Biology*, *25*(3), 1025–1040. https://doi.org/10.1128/MCB.25.3.1025-1040.2005
104. Moll, U. M., Marchenko, N., & Zhang, X.-K. (2006). p53 and Nur77/TR3 - transcription factors that directly target mitochondria for cell death induction. *Oncogene*, *25*(34), 4725–4743. https://doi.org/10.1038/sj.onc.1209601
105. Marchenko, N. D., Zaika, A., & Moll, U. M. (2000). Death Signal-induced Localization of p53 Protein to Mitochondria A POTENTIAL ROLE IN APOPTOTIC SIGNALING*. *The Journal of Biological Chemistry*, *275*(21), 16202–16212. https://doi.org/10.1074/jbc.275.21.16202
106. Abcam. Sample preparation for western blot. http://www.abcam.com/protocols/sample-preparation-for-western-blot
107. Wu, Y. C., Wu, W. K. K., Li, Y., Yu, L., Li, Z. J., Wong, C. C. M., … Cho, C. H. (2009). Inhibition of macroautophagy by bafilomycin A1 lowers proliferation and induces apoptosis in colon cancer cells. *Biochemical and Biophysical Research Communications*, *382*(2), 451–456. https://doi.org/10.1016/j.bbrc.2009.03.051
108. Cmielova, J., & Rezacova, M. (2011). p21Cip1/Waf1 protein and its function based on a subcellular localization [corrected]. *Journal of Cellular Biochemistry*, *112*(12), 3502–3506. https://doi.org/10.1002/jcb.23296
109. Celllular Engineering Technologies (CET) Inc. Human Hepatocellular Carcinoma (HepG2) Cells. HEPG2-500. http://search.cosmobio.co.jp/cosmo_search_p/search_gate2/docs/CET_/HEPG2500.20110706.pdf
110. Wilkening, S., Stahl, F., & Bader, A. (2003). Comparison of primary human hepatocytes and hepatoma cell line HepG2 with regard to their biotransformation properties. *Drug Metabolism and Disposition*, *31*(8), 1035 LP-1042. http://dmd.aspetjournals.org/content/31/8/1035
111. Beckerman, R., & Prives, C. (2010). Transcriptional Regulation by P53. *Cold Spring Harbor Perspectives in Biology*, *2*(8), a000935. https://doi.org/10.1101/cshperspect.a000935
112. Feng, Z., Zhang, H., Levine, A. J., & Jin, S. (2005). The coordinate regulation of the p53 and mTOR pathways in cells. *Proceedings of the National Academy of Sciences of the United States of America*, *102*(23), 8204–8209. https://doi.org/10.1073/pnas.0502857102
113. Day, D. A., & Tuite, M. F. (1998). Post-transcriptional gene regulatory mechanisms in eukaryotes: an overview. *The Journal of Endocrinology*, *157*(3), 361–371.

114.He, C., & Klionsky, D. J. (2009). Regulation mechanisms and signaling pathways of autophagy. *Annual Review of Genetics*, *43*, 67–93. https://doi.org/10.1146/annurev-genet-102808-114910
115.Balaburski, G., Budina, A., & Murphy M., (2013) Oncogenes and Tumor Suppressor Genes in Autophagy. Autophagy Cancer 8: 133-138
116.Feng, Z., Hu, W., De Stanchina, E., Teresky, A. K., Jin, S., Lowe, S., & Levine, A. J. (2007). The regulation of AMPK beta 1, TSC2, and PTEN expression by p53: Stress, cell and tissue specificity, and the role of these gene products in modulating the IGF-1-AKT-mTOR pathways. Cancer Research, 67(7), 3043–3053. https://doi.org/10.1158/0008-5472.CAN-06-4149
117.Kim, Y. C., & Guan, K. L. (2015). MTOR: A pharmacologic target for autophagy regulation. *Journal of Clinical Investigation*, *125*(1), 25–32. https://doi.org/10.1172/JCI73939
118.Sengupta, S., Peterson, T. R., & Sabatini, D. M. (2010). Regulation of the mTOR complex 1 pathway by nutrients, growth factors, and stress. *Molecular Cell*, *40*(2), 310–322. https://doi.org/10.1016/j.molcel.2010.09.026
119.Alers, S., Löffler, A. S., Wesselborg, S., & Stork, B. (2012). Role of AMPK-mTOR-Ulk1/2 in the Regulation of Autophagy: Cross Talk, Shortcuts, and Feedbacks. Molecular and Cellular Biology, 32(1), 2–11. http://doi.org/10.1128/MCB.06159-11
120.Lee, J. W., Park, S., Takahashi, Y., & Wang, H. G. (2010). The association of AMPK with ULK1 regulates autophagy. *PLoS ONE*, *5*(11), 1–9. https://doi.org/10.1371/journal.pone.0015394
121.Alers, S., Löffler, A. S., Wesselborg, S., & Stork, B. (2012). Role of AMPK-mTOR-Ulk1/2 in the Regulation of Autophagy: Cross Talk, Shortcuts, and Feedbacks. *Molecular and Cellular Biology* , *32*(1), 2–11. https://doi.org/10.1128/MCB.06159-11
122.Kroemer, G., Mariño, G., & Levine, B. (2010). Autophagy and the Integrated Stress Response. Molecular Cell, 40(2), 280–293. http://dx.doi.org/10.1016/j.molcel.2010.09.023
123.Hardie, D. G. (2011). AMPK and autophagy get connected. *Embo J*, *30*(4), 634–635. https://doi.org/10.1038/emboj.2011.12
124.Kim, J., Kundu, M., Viollet, B., & Guan, K.-L. (2011). AMPK and mTOR regulate autophagy through direct phosphorylation of Ulk1. *Nature Cell Biology*, *13*(2), 132–141. https://doi.org/10.1038/ncb2152
125.Egan, D. F., Shackelford, D. B., Mihaylova, M. M., Gelino, S., Kohnz, R. A., Mair, W., … Shaw, R. J. (2011). Phosphorylation of ULK1 (hATG1) by AMP-activated protein kinase connects energy sensing to mitophagy. *Science (New York, N.Y.)*, *331*(6016), 456–461. https://doi.org/10.1126/science.1196371
126.Hoyer-Hansen, M., Bastholm, L., Szyniarowski, P., Campanella, M., Szabadkai, G., Farkas, T., … Jaattela, M. (2007). Control of macroautophagy by calcium, calmodulin-dependent kinase kinase-beta, and Bcl-2. *Molecular Cell*, *25*(2), 193–205. https://doi.org/10.1016/j.molcel.2006.12.009
127.Hardie, D. G. (2004). The AMP-activated protein kinase pathway – new players upstream and downstream. *Journal of Cell Science*, *117*(23), 5479 LP-5487. http://jcs.biologists.org/content/117/23/5479
128.Okoshi, R., Ozaki, T., Yamamoto, H., Ando, K., Koida, N., Ono, S., … Kizaki, H. (2008). Activation of AMP-activated protein kinase induces p53-dependent apoptotic cell death in response to energetic stress. *Journal of Biological Chemistry*, *283*(7), 3979–3987. https://doi.org/10.1074/jbc.M705232200
129.Ng, S., Wu, Y.-T., Chen, B., Zhou, J., & Shen, H.-M. (2011). Impaired autophagy due to constitutive mTOR activation sensitizes TSC2-null cells to cell death under stress. *Autophagy*, *7*(10), 1173–1186. https://doi.org/10.4161/auto.7.10.16681

130. Levine, A., Feng, Z., Mak, T., You, H., & Jin, S. (2006). Coordination and communication between the p53 and IGF-I-AKT-TOR signal transduction pathways. *Genes & Development*, (609), 267–275. https://doi.org/10.1101/gad.1363206
131. Liu, K., Shi, Y., Guo, X. H., Ouyang, Y. B., Wang, S. S., Liu, D. J., … Chen, D. X. (2014). Phosphorylated AKT inhibits the apoptosis induced by DRAM-mediated mitophagy in hepatocellular carcinoma by preventing the translocation of DRAM to mitochondria. *Cell Death & Disease*, *5*, e1078. https://doi.org/10.1038/cddis.2014.51
132. Crighton, D., Wilkinson, S., O'Prey, J., Syed, N., Smith, P., Harrison, P. R., … Ryan, K. M. (2017). DRAM, a p53-Induced Modulator of Autophagy, Is Critical for Apoptosis. *Cell*, *126*(1), 121–134. https://doi.org/10.1016/j.cell.2006.05.034
133. Zhang, X.-D., Qi, L., Wu, J.-C., & Qin, Z.-H. (2013). DRAM1 Regulates Autophagy Flux through Lysosomes. *PLoS ONE*, *8*(5), e63245. https://doi.org/10.1371/journal.pone.0063245
134. Crighton, D., Wilkinson, S., & Ryan, K. M. (2007). DRAM links autophagy to p53 and programmed cell death. Autophagy, 3(1), 72–74. http://dx.doi.org/10.4161/auto.3438
135. Ravikumar, B., Sarkar, S., Davies, J. E., Futter, M., Garcia-Arencibia, M., Green-Thompson, Z. W., … Rubinsztein, D. C. (2010). Regulation of mammalian autophagy in physiology and pathophysiology. *Physiological Reviews*, *90*(4), 1383–435. https://doi.org/10.1152/physrev.00030.2009.
136. Brown, E. J., Beal, P. A., Keith, C. T., Chen, J., Shin, T. B., & Schreiber, S. L. (1995). Control of p70 s6 kinase by kinase activity of FRAP in vivo. *Nature*, *377*(6548), 441–446. https://doi.org/10.1038/377441a0
137. Xu, Y., Parmar, A., Roux, E., Balbis, A., Dumas, V., Chevalier, S., & Posner, B. I. (2012). Epidermal Growth Factor-induced Vacuolar (H+)-ATPase Assembly: A Role in Signaling via mTORC1 Activation. *Journal of Biological Chemistry*, *287*(31), 26409–26422. https://doi.org/10.1074/jbc.M112.352229
138. Thoreen, C. C., Kang, S. A., Chang, J. W., Liu, Q., Zhang, J., Gao, Y., … Gray, N. S. (2009). An ATP-competitive mammalian target of rapamycin inhibitor reveals rapamycin-resistant functions of mTORC1. *The Journal of Biological Chemistry*, *284*(12), 8023–8032. https://doi.org/10.1074/jbc.M900301200
139. Kwon, S., Jeon, J.-S., Ahn, C., Sung, J.-S., & Choi, I. (2016). Rapamycin regulates the proliferation of Huh7, a hepatocellular carcinoma cell line, by up-regulating p53 expression. Biochemical and Biophysical Research Communications, 479(1), 74–79. http://dx.doi.org/10.1016/j.bbrc.2016.09.035
140. Law, B. K. (2005). Rapamycin: an anti-cancer immunosuppressant? *Critical Reviews in Oncology/hematology*, *56*(1), 47–60. https://doi.org/10.1016/j.critrevonc.2004.09.009
141. Yan, Y., Jiang, K., Liu, P., Zhang, X., Dong, X., Gao, J., … Gong, P. (2016). Bafilomycin A1 induces caspase-independent cell death in hepatocellular carcinoma cells via targeting of autophagy and MAPK pathways. *Scientific Reports*, *6*, 37052. https://doi.org/10.1038/srep37052
142. Newton, P. T., Vuppalapati, K. K., Bouderlique, T., & Chagin, A. S. (2015). Pharmacological inhibition of lysosomes activates the MTORC1 signaling pathway in chondrocytes in an autophagy-independent manner. *Autophagy*, *11*(9), 1594–1607. https://doi.org/10.1080/15548627.2015.1068489
143. Vaux, D. L. (2012). Research methods: Know when your numbers are significant. *Nature*, *492*(7428), 180–181. http://dx.doi.org/10.1038/492180a
144. Yang, Z. J., Chee, C. E., Huang, S., & Sinicrope, F. A. (2011). The Role of Autophagy in Cancer: Therapeutic Implications. *Molecular Cancer Therapeutics*, *10*(9), 1533 LP-1541. http://mct.aacrjournals.org/content/10/9/1533
145. Sullivan, M. A., Harcourt, B. E., Xu, P., Forbes, J. M., & Gilbert, R. G. (2015). Impairment of Liver Glycogen Storage in the db/db Animal Model of Type 2 Diabetes:

A Potential Target for Future Therapeutics? Current Drug Targets, 16(10), 1088–1093. http://www.eurekaselect.com/133505/article
146. Rambold, A. S., Cohen, S., & Lippincott-Schwartz, J. (2015). Fatty acid trafficking in starved cells: regulation by lipid droplet lipolysis, autophagy, and mitochondrial fusion dynamics. *Developmental Cell*, *32*(6), 678–692. https://doi.org/10.1016/j.devcel.2015.01.029
147. Welte, M. A. (2015). Expanding roles for lipid droplets. *Current Biology: CB*, *25*(11), R470–R481. https://doi.org/10.1016/j.cub.2015.04.004
148. Czaja, M. J., & Cuervo, A. M. (2009). Lipases in lysosomes, what for? *Autophagy*, *5*(6), 866–867. http://www.ncbi.nlm.nih.gov/pmc/articles/PMC3643983/
149. Singh, R., & Cuervo, A. M. (2011). Autophagy in the Cellular Energetic Balance. *Cell Metabolism*, *13*(5), 495–504. https://doi.org/10.1016/j.cmet.2011.04.004
150. Eskelinen, E. L., & Kovács, A. L. (2011). Double membranes vs. lipid bilayers, and their significance for correct identification of macroautophagic structures. *Autophagy*, *7*(9), 931–932. https://doi.org/10.4161/auto.7.9.16679
151. Badadani, M., (2012). Autophagy Mechanism, Regulation, Functions, and Disorders. ISRN Cell Biology, 2012, Volume 2012 (2012), Article ID 927064, 11 pages. http://dx.doi.org/10.5402/2012/927064
152. Schneider, J. L., & Cuervo, A. M. (2014). Liver Autophagy: much more than just taking out the trash. *Nature Reviews. Gastroenterology & Hepatology*, *11*(3), 187–200. https://doi.org/10.1038/nrgastro.2013.211
153. Ding, W. X., & Yin, X. M. (2009). *Chapter 20 Analyzing Macroautophagy in Hepatocytes and the Liver*. *Methods in Enzymology* (1st ed., Vol. 453). Elsevier Inc. https://doi.org/10.1016/S0076-6879(08)04020-2
154. Mizushima, N., Yamamoto, A., Matsui, M., Yoshimori, T., & Ohsumi, Y. (2004). In Vivo Analysis of Autophagy in Response to Nutrient Starvation Using Transgenic Mice Expressing a Fluorescent Autophagosome Marker. *Molecular Biology of the Cell*, *15*(3), 1101–1111. https://doi.org/10.1091/mbc.E03-09-0704
155. Ezaki, J., Matsumoto, N., Takeda-Ezaki, M., Komatsu, M., Takahashi, K., Hiraoka, Y., … Ueno, T. (2011). Liver autophagy contributes to the maintenance of blood glucose and amino acid levels. *Autophagy*, 7(7), 727–736. http://doi.org/10.4161/auto.7.7.15371

7 Appendix

7.1 Cell culture protocols

7.1.1 Primary human hepatocytes

Primary human hepatocytes were thawed and seeded according to the manufacturer's instructions (QPS Hepatic Bioscience).

-Materials and Preparations:

- Cryopreserved Recovery Medium (CRM050)

25ml of CRM were added to 25 ml PBS to get a final volume of 50 ml, which is necessary to dilute DMSO properly. The complete medium was stored at -20°C.

- Cryopreserved Plating Medium (CPM250)

CPM medium was completed by adding following supplements:

25 ml	FBS
2,5 ml	Sodium Pyruvate
2,5 ml	Penicillin/Streptromycin
250 µl	Insulin
25 µl	Dexamethasone

Noteworthy, 50 µl instead of 25 µl Dexamethasone was added to the medium by accident. However, the higher concentration did not seem to interfere with the plating capacity of the cells. An aliquot of the complete medium was sterile filtered (0,2 µm filter) and stored at 4°C

- Cryopreserved Maintenance Medium (CMM250)

CMM medium was completed by adding 2,5 ml CMM Supplement Pack and 2,5 µl Dexamethasone. An aliquot of the complete medium was sterile filtered (0.2 µm filter) and stored at 4°C.

-Thawing and plating:

CRM and CPM were pre-warmed to 37°C in a water bath. The cryopreserved primary human hepatocytes were transferred from the nitrogen liquid storage to a water bath by using a cryogenic container. The cells were thawed in the water bath for 90 – 120 seconds until only a small ice crystal remained in the vial. Once thawed, the vial was placed into wet ice before moving them into the laminar flow. Then, the vial was poured directly into warmed CRM (50 ml). The vial was washed three times with medium in order to rinse residual cells from the vial. The cell suspension was mixed by gently inverting the centrifuge tube and subsequently centrifuged at 100xg for 8 min on RT. Carefully, the supernatant was removed and the cell pellet was gently resuspended in 5ml of warmed CPM by gently rocking the tube back and forth. Then, the cell viability and yield was determined using Trypan Blue exclusion. The cells were then seeded on collagen I-coated plates according to the manufacture's recommendations (24-well plate: 0,7 – 0,9 x 10^6 cells/ml). The seeded plate was then placed into the incubator (37°C/ 5% CO^2) and was gently shaken 4x North to South and 4x East to West in order to distribute the cells evenly. The shaking was repeated three times before the cells could settle and attach. To ensure that dead cells lift from the plate, the whole procedure was repeated every 15 min for one hour. The cells were then incubated overnight. Noteworthy, the plate should not move during this time, as the cells were forming a monolayer. One day after plating, the CPM medium was changed to CMM medium. The experiment was done three days after plating.

7.1.2 HepaRG cell line

Cryopreserved HepaRG cells were thawed and cultured according to manufacture's user guide (ThermoFisher Scientific). Noteworthy, this protocol is based on a single vial containing 10^7 cells, which are terminally differentiated and used for endpoint experiments. This protocol is not suitable for subculturing HepaRG cells.

-Materials and Preparations:

- HepaRG Thaw, Plate, & General Purpose Medium (HRPG670)

5,6 ml HepaRG Supplement was added to 40 ml William' Medium E and 40 µl GlutaMAX. The complete medium was stored at 4°C until further use.

- HepaRG Maintenance/Metabolism Medium (HRPG620)

Working medium was prepared by adding the entire contents of the bottle of HepaRG Supplement (16 ml) to 100 ml William' Medium E and 1 ml GlutaMAX. The complited medium was aliquoted and stored at 4°C. The complete medium was pre-warmed at RT prior use.

-Thawing and plating:

HepaRG Thaw, Plate, & General Purpose Medium was pre-warmed to 37°C in a water bath. 9 ml of the warmed medium was then added into a centrifuge tube. The cryopreserved HepaRG cells were removed from the nitrogen liquid storage and were thawed in the water bath for 1 – 2 minutes until only a small ice crystal remained in the vial. Then, the vial was poured directly into the tube containing 9 ml of thrawing medium, resulting in a 1:10 ratio of cell suspeonsion. The vial was washed once with medium in order to rinse residual cells from the vial. The cell suspension was mixed by gently inverting the centrifuge tube and subsequently centrifuged at 400 x g for 2 min on RT. Carefully, the supernatant was removed and the cell pellet was resuspended in 5ml of warmed thrawing medium. Then, the cell viability and yield was determined using Trypan Blue exclusion. The cells were then seeded on collagen I-coated plates according to the manufacture's recommendations (24-well plate: 1,2 x 106 cells/ml). The seeded plate was then placed into the incubator (37°C/ 5% CO2) and was gently shaken 4x North to South and 4x East to West in order to distribute the cells evenly. The cell morphology was observed under light microscope 4 hours after plating. One day after thawing, the thawing medium was replaced by the complete HepaRG Maintenance/Metabolism Medium. The medium was renewed on day 5 and day 7 after thawing. The starvation experiment was done after one week in culture.

7.1.3 Upcyte Hepatocytes

Cryopreserved Upcyte Hepatocytes were thawed and cultured according to manufacture's instructions (Upcyte technologies).

-Materials and Preparations:

- Hepatocyte Thawing Medium

The ready-to-use thawing medium was stored at 4°C until further use.

- Hepatocyte High Performance Medium (Endpoint Medium)

The ready-to-use thawing medium was stored at 4°C until further use.

- Trypsin Stop Solution

High Performance Medium containing 10% fetal bovine serum.

-Thawing and plating:
Hepatocyte Thawing Medium was pre-warmed to 37°C in a water bath. The cryopreserved hepatocytes were transferred from the nitrogen liquid storage to a water bath. The cells were thawed in the water bath for a few seconds until all ice had disappeared in the vial. Then, the vial was poured directly into warmed thawing medium (50 ml). The vial was washed twice with medium in order to rinse residual cells from the vial. The cell suspension was centrifuged at 100xg for 5 min on RT. Carefully, the supernatant was removed, leaving 200 – 400 µl of the medium on top of the pellet. The pellet was gently loosened and resuspended by rotating the tube. 2 ml of pre-warmed High Performance Medium was then added to the cell suspension (1 ml per million cells thawed). Pipetting the cells up and down should be avoided. The cell viability and yield was determined using Trypan Blue exclusion. The cells were then seeded on collagen I-coated flasks according to the manufacture's recommendations (10,000 cells/ cm2). The cells were cultured until they had reached 70-80% confluence. The medium was renewed every 2 – 3 days. 5 days after plating, the cells were ready to be passaged. Subsequently, Hepatocyte Medium was prewarmed to RT. The cells were washed with once with PBS (100 µl PBS/cm2) and once with 1x Trypsin (0,05%/0,02% EDTA, 100 µl/cm2). The cells were incubated with 1x Trypsin (100 µl/cm2) and incubated up to 10 min at 37°C, according to the manufacture's recommendations. Then, twice the volume of High Performance Medium (200 µl/cm2) containing 10% fetal bovine serum was added to stop the Trypsin activity. The cell suspension was transferred into a tube and centrifuged at 100x for 5 min at RT. The cells were then seeded on collagen I-coated plates according to the manufacture's recommendations (150.000 cells/ cm2). The cells were cultured for 3 days.
However, the passaging did not work and only a few cells were transferred into the culture dishes, whereas the old flaks were about 100% confluent. Therefore, the seeding step was repeated on day 8 after thawing. The cells were washed with PBS and 1x Trypsin. Then, 1x Trypsin (3,5 ml Trypsin per T75 flask) was added and incubated for 5 min. Twice the volume of High Performance Medium containing 10% fetal bovine serum was added to stop the Trypsin activity. The cells were centrifuged at 100xg for 5 min and seeded at 80.000 cells/cm2 in High Performance Medium in a collagen type I coated 12-well plate. The cells were then cultured for three days and the medium was renewed on day 9 and 11. 15 days after thawing, the starvation experiment was done.

7.2 Supplementary information

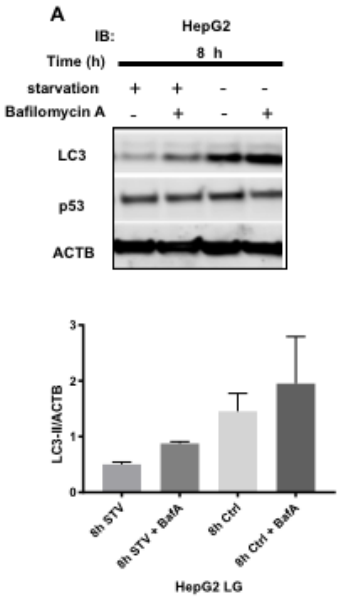

Figure S1: Monitoring Autophagy in HepG2 cells cultured in low glucose medium. HepG2 cells were cultured in starvation medium or normal growth medium and treated with 10 nM Bafilomycin A1 or DMSO as vehicle control. Treatment was added 2h prior harvest. Western blot analysis of p53, LC3 and ACTB in HepG2 cells after 8h of cultivation. ACTB served as loading controls (n=2)

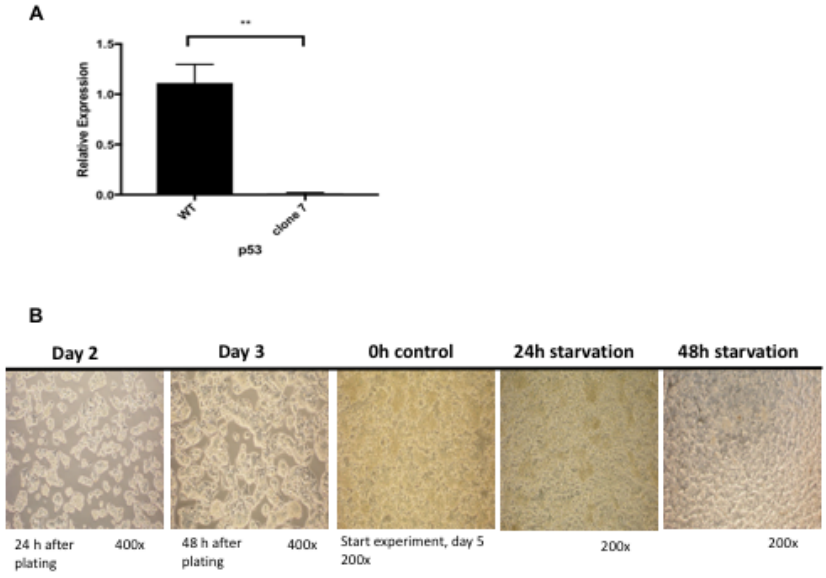

Figure S2: stable p53 knockout in HepG2 clone 7 cells. HepG2 clone 7 cells were subjected to starvation medium for 24h and treated with 10 nM Bafilomycin A1 or DMSO as vehicle control. Treatment were added 2h prior harvest. **(A)** qPCR analysis of p53 in wildtype HepG2 (p53 +/+) and HepG2 clone 7 cells (p53 -/-) after 48h of starvation (n=3). Expression levels were normalized to GAPDH as internal housekeeping gene. **(B)** Cell morphology of HepG2 Clone 7 cells from day of seeding till end of the experiment.